

THESIS FOR THE DEGREE OF LICENTIATE OF ENGINEERING

**Steam Cracking of Polyolefins in Fluidized Bed Systems: Influences of the
Bed Materials on the Hydrogen Transfer Reactions**

CHAHAT MANDVIWALA

Department of Space, Earth and Environment

CHALMERS UNIVERSITY OF TECHNOLOGY

Gothenburg, Sweden 2022

Steam Cracking of Polyolefins in Fluidized Bed Systems: Influences of the Bed Materials on the Hydrogen Transfer Reactions

CHAHAT MANDVIWALA

© CHAHAT MANDVIWALA, 2022.

Department of Space, Earth and Environment

Chalmers University of Technology

SE-412 96 Gothenburg

Sweden

Telephone + 46 (0)31-772 1432

Printed by Chalmers Reproservice

Gothenburg, Sweden 2022

Steam Cracking of Polyolefins in Fluidized Bed Systems: Influences of the Bed Materials on the Hydrogen Transfer Reactions

CHAHAT MANDVIWALA
Division of Energy Technology
Department of Space, Earth and Environment
Chalmers University of Technology

Abstract

Plastic materials are crucial to the supply of everyday necessities, such as clothes, packaging, and building materials. Most plastic materials are disposed of after a short period of use due to their low cost of production. The linear use of plastics has resulted in high levels of plastic waste materials. In addition, the production of plastics is largely dependent upon fossil resources. A paradigm shift in relation to the production and management of plastic waste is necessary for the development of a sustainable plastic usage.

Plastic waste is challenging to recycle, given its inherent heterogeneous nature. In this context, recycling using thermochemical processes is a promising approach towards fossil-free production of new plastics of original quality from the abundantly available plastic waste. For this application, steam cracking in a dual fluidized bed (DFB) reactor is a suitable process owing to its flexibility. This work focuses on strengthening the position of the DFB steam cracking technology in the recycling of plastic waste. Experimental studies were conducted on steam cracking of polyethylene, a polyolefin, and rapeseed oil, a polyolefin-like feedstock, in a laboratory reactor under operating conditions similar to that of a DFB system. The suitability of such feedstocks for the DFB steam cracking process is discussed with respect to the distribution of the obtained products. The influence of the bed material on the steam cracking reactions of polyolefins is also examined.

The results presented in this thesis demonstrate that steam cracking in a DFB system is a suitable process for the recycling of polyolefin and polyolefin-type feedstocks. Steam cracking of such feedstocks yields a product distribution that is similar to that obtained from thermal cracking of petroleum naphtha. Experiments investigating the influences of the bed material on the steam cracking reactions reveal that the activity of the bed material towards the hydrogen transfer (C-H bond scission) reactions is a critical parameter for the process.

An increase in the catalytic activity of the bed material towards the hydrogen transfer reactions results in either dehydrogenation or hydrogenation of the polyolefin feedstock. Dehydrogenation is associated with the oxidizing nature of the bed material, and results in the formation of compounds with H/C ratios <2 . In contrast, hydrogenation promoted by the bed material leads to the enhanced formation of compounds with H/C ≥ 2 . Hydrogenation was observed in the presence of a reduced bed material and was associated with the water dissociation and hydrogen transfer capabilities of the bed material. Extensive experimental results supporting these findings are discussed throughout the thesis.

Keywords: Plastic waste, steam cracking, dual fluidized bed, polyolefins, hydrogen transfer

List of publications included in this thesis

This thesis is based on the following three appended papers, which are referred to in the text according to their Roman numerals:

Paper I

Mandviwala. C., Berdugo Vilches. T., Seemann. M., Faust. R., Thunman. H.

Thermochemical conversion of polyethylene in a fluidized bed: Impact of transition metal-induced oxygen transport on product distribution

Journal of Analytical and Applied Pyrolysis, 163 (2022) 105476

Paper II

Mandviwala. C., Berdugo Vilches. T., Seemann. M., González-Arias. J., Thunman. H.

Unraveling the hydrocracking capabilities of fluidized bed systems operated with natural ores as bed materials

Manuscript submitted to Journal of Analytical and Applied Pyrolysis (2022)

Paper III

Mandviwala. C., González-Arias. J., Seemann. M., Berdugo Vilches. T., Thunman. H.

Fluidized bed steam cracking of rapeseed oil: exploring the direct production of the molecular building blocks for the plastics industry

Manuscript submitted to Biomass Conversion and Biorefinery (2022)

Chahat Mandviwala is the principal author of **Papers I–III** and conducted the experimental measurements, data processing, interpretation of the results and authorship of the manuscripts. Associate Professor Martin Seemann, who is the main academic supervisor, contributed with discussions and editing to **Papers I–III**. Co-supervisors Professor Henrik Thunman and Dr. Teresa Berdugo Vilches also contributed to the discussions and editing of **Papers I–III**. Robin Faust assisted with the experimental measurements performed for **Paper I**. Dr. Judith González-Arias assisted with the experimental measurements, data processing and editing the manuscript for **Papers II** and **III**.

ACKNOWLEDGMENTS

I would not be writing this if it weren't for some important people in my life. My PhD journey, so far, has been made enjoyable by many wonderful people who have guided me and accompanied me. Beginning with my supervisor, Martin Seemann, I would like to thank Martin for his guidance and support since my first day at Chalmers. My life would have been difficult without his enthusiasm and witty jokes.

I would also like to thank my co-supervisors Henrik Thunman and Teresa Berdugo Vilches for their guidance and support. I am grateful to Henrik for always showing me the way forward whenever I felt I was at a dead-end. Apart from the research talks, it has always been a pleasure to hear Henrik's life stories and I hope he has some more to tell. Special thanks to Teresa for being a great teacher and mentor. I will admit that the first year of my PhD without Teresa in the group was a bit difficult. I would also like to thank her for creating a truly amazing work environment at the Chalmers *Kraftcentralen*.

I have had the privilege to spend the cold winter days in one of the warmest places in Sweden: *Kraftcentralen* (KC). All thanks to our 'unsung heroes' – the research engineers – Jessica Bohwalli, Johannes Öhlin, and Rustan Hvitt for creating this world-class experimental infrastructure. I would also like to thank the operating staff at Akademiska Hus: Jelena, Isabel, Petrus, and Mikael for the operation of the boiler. Thanks a lot for your patience and for making that 'one more low-temperature point' possible.

I am also grateful to the rest of the gasification group or as we say now 'Junior Crackers': Isabel, Sébastien, Judith, Rene and Tharun for making this research group exceptional. I would like to thank Isabel, Judith and Rene for making the experiments possible in KC and in the lab. I must say that experiments were never as much fun without Judith in the group.

Apart from the gasification group, I would like to thank all the PhD students at Energy Technology for creating a friendly and collaborative atmosphere. I am also grateful to all of you for keeping my social life alive.

Finally, I would like to thank my parents for their love and support, as without them I would never have enjoyed so many opportunities.

Chahat Mandviwala, Gothenburg 2022

ahimsā paramo dharma

Contents

1 – Introduction	1
1.1 Motivation	1
1.2 Aim and scope of this thesis	4
1.3 Contribution to this thesis.....	5
1.4 Outline of this thesis.....	5
2 – The Landscape	6
2.1 Thermochemical recycling principle.....	6
2.2 Steam cracking.....	8
2.2.1 Feedstocks with the polyolefin-type molecular structure	8
2.2.2 Reactions governing the steam cracking of polyolefins	10
2.3 Steam cracking in the DFB reactor configuration.....	14
3 – Experimental Setup.....	18
3.1 Description of the BFB steam cracker.....	18
3.2 Feedstocks and bed materials.....	19
3.3 Chemical looping tests	21
3.4 Blank water dissociation test	22
3.5 Steam cracking tests.....	23
3.6 Hydrocracking tests.....	25
4 – Data Processing and Analysis.....	26
5 – Results and discussion.....	29
5.1 Properties of the bed materials.....	29
5.2 Carbon balance.....	33
5.3 Suitability of the feedstock	36
5.3.1 Polyethylene.....	36
5.3.2 Vegetable oil	36
5.4 H/C ratio of the products	38
5.4.1 Dehydrogenation by the bed materials	39
5.4.2 Hydrogenation by the bed material	41
6 – Summary and Conclusions.....	44
Recommendations for future work	46
Nomenclature.....	47
References	48

CHAPTER 1

1 – Introduction

1.1 Motivation

Plastics are advanced materials that provide Society with essential products and services. The extremely low production cost of plastics has led to their extensive application in medical products, foodstuffs, transportation, and many other industrial products. The widespread usage of plastics has caused a steady increase in plastic production over the last few decades, reaching a global production level of 368 metric million tonnes (MMT) in 2019.¹

Plastics are manufactured from monomers or molecular building blocks, by means of various polymerization processes. Currently, the molecular building blocks used to manufacture plastics, such as ethylene, propylene, butadiene, benzene, and styrene, are derived from fossil-based resources. These molecular building blocks are obtained by thermal cracking or steam cracking of petroleum naphtha, gas-oil or liquefied petroleum gas (LPG). These processes account for 4%–6% of the global fossil resource consumption.² Furthermore, due to the low cost of plastic production, plastics quickly become waste materials. The most commonly generated plastic wastes constitute a serious waste-handling problem due to their resistance to degradation. As of the Year 2015, approximately 6.3 billion tonnes of plastic waste had been generated, of which around 79% was dumped in landfills or in the natural environment, 12% was incinerated, and only 9% was recycled.³ If the current plastic production and waste management trends continue, approximately 12 billion tonnes of plastic waste will be in the natural environment or landfills by the Year 2050.³ Therefore, fossil-based plastic production and the management of the generated plastic waste raise serious sustainability issues.

The European Union Waste Framework Directive (WFD) is a tool that prioritizes the order of operations to be followed in waste management as follows: prevention, re-use, recycling, energy recovery, and disposal.⁴ Despite this Directive, a major part of the generated plastic waste is currently disposed of, landfilled, or lost to the environment.³ Although prevention is

regarded as the highest priority, a world without plastics seems unimaginable today. Similarly, the re-use of the majority of the plastics, particularly those used in the medical field and food industry, is challenging. Moreover, the best possible re-use of plastics can meet only a fraction of the total plastic demand. Recycling and energy recovery present two suitable options for the treatment of the abundantly generated plastic waste. Although energy recovery is a viable option, it does not provide a solution for the sustainable production of plastics. Therefore, in this case, recycling plastic waste into new plastics is the preferred option for a sustainable economy using plastics.

When it comes to recycling plastic waste, mechanical recycling seems to be a suitable approach at first glance. As of today, recycling of plastic waste is predominantly based on mechanical methods.^{2,3} However, mechanical recycling is only suitable for highly homogeneous plastic waste. Recycling through mechanical methods is complicated by the presence of impurities (e.g., paper, cardboards, metals, etc.) in the plastic waste. Advanced sorting and cleaning of plastic waste is crucial for mechanical recycling methods. Mechanical recycling of plastics also requires several steps before the plastic can be used again for the same purpose. For example, mechanical recycling of well-sorted PET bottles involves 17 steps.⁵ In addition, the inherent properties of the polymer limit the number of times that plastic can be mechanically recycled. That implies that even with the use of advanced sorting systems, mechanical recycling of plastic waste will be limited, and the recycling will entail degradation of the properties of the original plastic material.²

Progression towards a sustainable plastic-using economy requires the use of plastic materials in a circular way. Recycling methods that produce any type of new plastic of the same quality as the original from any type of plastic waste (sorted or unsorted) could lead to the achievement of this goal. Thermochemical recycling of plastic waste, where the focus is on producing the molecular building blocks of plastics from plastic waste, is preferable in this case. Conversion of plastic waste into its molecular building blocks theoretically enables unlimited recycling of any plastic material. Such recycling methods can be applied to any type of plastic waste, regardless of the availability of advanced sorting systems. In addition, thermochemical recycling provides flexibility in terms of the feedstock and product distribution, which makes the recycling system adaptable to changes in consumption and production patterns. For these reasons, thermochemical recycling can act as a bridge between waste management and the production of plastics. The development of such recycling methods will not only help solve the plastic waste problem, but will also allow the plastic manufacturing industry to become independent of fossil reserves.

A more resource-efficient way of handling plastic waste will contribute to the transition towards a circular economy. Such a plastic-using economy will face a feedstock deficit resulting from the ever-increasing demand for plastics and unrecoverable losses to the environment. Therefore, there will still be a need for virgin fossil feedstocks to compensate for the feedstock deficit. However, in a scenario in which stringent climate mitigation rules have phased out the use of fossil-based carbon, it seems reasonable to look for alternative feedstocks. Biogenic wastes, in this case, can provide the possibility to replace virgin fossil feedstocks and compensate for the feedstock deficit.

Anthropogenic waste streams that are rich in plastics, the new feedstock for the plastic industry, are more complex than the fossil-based feedstocks that we have exploited until now. These waste streams are expected to be a heterogeneous mixture of biogenic and inorganic wastes, such as paper, cardboard and metals. The conversion reactions of various types of polymers and biomass occur at different temperatures in the thermochemical reactor. Moreover, the contaminants present in the waste can lead to the formation of pollutants and corrosive substances during their thermochemical conversion. A thermochemical recycling method that overcomes these challenges is, therefore, required.

In this context, fluidized bed steam cracking has certain characteristics that make it suitable for the thermochemical recycling of plastic waste. A fluidized bed reactor is deemed suitable for the conversion of plastic waste due to its heat transfer properties and its ability to handle heterogeneous feedstocks. The heat transfer and mixing properties of a fluidized bed ensure high heating rates, thereby minimizing hotspots and enabling operational control of the reactions.⁶ In addition, using steam as the exclusive fluidization agent for steam cracking leads to the production of a nitrogen-free product gas, as is obtained from steam cracking of fossil-based feedstocks.^{2,7} Experience gained over three decades of research into fluidized bed steam cracking of plastics reveals that the products derived from this process are comparable to those derived from the steam cracking of naphtha, a fossil-based feedstock.^{2,6-8}

The formation of carbon deposits from liquid and gaseous hydrocarbons in the steam cracking process is a common phenomenon.⁹ In a fluidized bed process, this will lead to the formation of solid carbon, either as char or as carbon deposits on the bed material surface. The reactor configuration should be selected to be sufficiently robust to remove the solid carbon deposits formed during the steam cracking process. The formation of solid carbon in fluidized beds during thermochemical reprocessing leads to loss of the fluid phase and loss of the heat transfer capacity of the fluidized bed.¹⁰ Although plastics have a negligible fixed carbon content, steam cracking of plastics in fluidized bed reactors is associated with significant formation of solid carbon in the bed material, as compared to the fixed carbon content.^{2,6-8,11} In addition, the presence of biogenic wastes in the feedstock will lead to the formation of solid carbon in the fluidized bed. For these reasons, continuous removal of the solid carbon formed in the fluidized bed is required. The removal of the carbon deposits in the industrial steam cracking and fluid catalytic cracking (FCC) processes is performed by exposing the carbon deposits to an oxidizing environment.⁹ In this sense, a dual fluidized bed (DFB) system has an advantage over standalone fluidized bed systems in that the solid carbon is removed continuously through oxidation within a secondary fluidized bed.

In DFB systems, hot bed material is recirculated between the interconnected fluidized beds, i.e., a steam-fluidized cracker and a regenerator, as illustrated in Figure 1. The heat required for steam cracking is transferred from the regenerator to the cracker by the bed material. This type of configuration, if sealed thoroughly, allows the production of two separate gas streams: flue gas from the regenerator; and nitrogen-free product gas from the steam cracker.

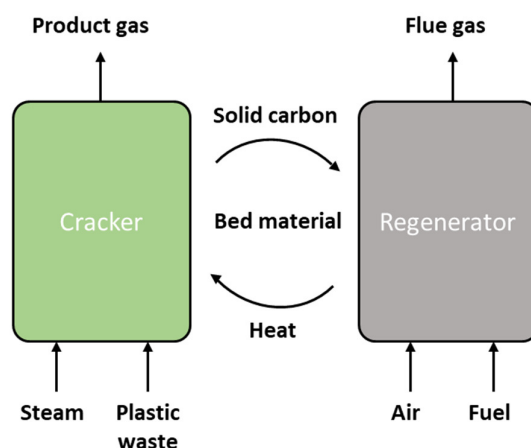


Figure 1. Setup of the dual fluidized bed steam cracker.

Notwithstanding its promising characteristics, DFB steam cracking of plastic waste has not yet been implemented at commercial scale. Moreover, research experience related to this process remains limited.^{2,7} Commercialization of any process depends on its cost-effectiveness. For a thermochemical process, this is usually associated with the conversion efficiencies and the yields of economically valuable products. Research activities related to DFB gasification of biomass over the last decade have revealed that the DFB configuration offers great flexibility regarding carbon conversion and product distribution.^{12,13} The distribution of products from a DFB steam cracker can, to a large extent, be tailored to specific requirements by adjusting the properties of the bed material, the reactor temperature, and the residence time. Steam cracking of polymers proceeds through a free radical-type reaction mechanism, and the final product distribution is known to be governed by the cracking (C-C bond scission) reactions and the hydrogen transfer (C-H bond scission) reactions.¹⁴⁻¹⁶ The importance of the bond scission reactions in the steam cracking of polymers is well-established.¹⁴⁻¹⁶ However, the influences of the operational conditions of the DFB configuration on these reactions remain largely unknown. There is, therefore, a need to explore the potential impacts of the DFB operational conditions on the cracking reactions and the hydrogen transfer reactions that occur during the steam cracking of plastics.

1.2 Aim and scope of this thesis

This work summarizes the results of investigations into the suitability of the DFB reactor configuration for the steam cracking of plastic and biogenic feedstocks, with the goal of strengthening its position as a plastic recycling technology in the circular economy. The present work also investigates the implications of the operational conditions of a DFB steam cracker for the steam cracking reactions. A particular aim of this thesis is to elucidate the influences of the bed material properties on the hydrogen transfer reactions that occur during the steam cracking of polyolefins.

At the inception of this work, there were no published papers on the influences of the operational conditions of the DFB configuration on the hydrogen transfer reactions that govern

the product distribution from steam cracking. The work conducted in this thesis focused on the following topics:

1. Evaluating the suitability of the DFB steam cracking process for feedstocks with polyolefin-type molecular structures.
2. Investigating the influence of oxygen transfer induced by the transition metal oxide content of the bed material on the hydrogen transfer reactions.
3. Determining the hydrocracking capabilities, through hydrogenation by steam, of DFB systems that are operated with natural ores as the bed materials.

1.3 Contribution to this thesis

Paper I of this thesis reveals the influence that the transition metal oxide content of the bed material exerts on the hydrogen transfer reactions during steam cracking of polyethylene in fluidized bed systems. This paper presents the first dataset establishing the exclusive impact of transition metal oxide-induced oxygen transfer on the reaction mechanism governing the steam cracking of polyolefins. **Paper II** elucidates the hydrocracking capabilities of fluidized beds operated with natural ores as bed materials. **Paper II** also presents a preliminary view of the hydrogen atom transfer from water to the hydrocarbon molecules that occurs in fluidized bed systems. In addition, this paper provides insights into the roles of the bed materials in the hydrocracking capabilities of fluidized beds. **Paper III** describes the importance of biogenic resources in the context of the circular utilization of plastics. This paper provides experimental data that establish waste cooking oil as a biogenic feedstock for the plastics industry, representing a potential alternative to crude oil.

1.4 Outline of this thesis

This thesis is based on the three appended papers (**Papers I–III**) and this introductory essay. Chapter 2 of the thesis introduces the principle of thermochemical recycling for the production of the molecular building blocks, and presents the theoretical background to the steam cracking of polyolefins. Chapter 3 outlines the experimental setup, the materials used, and the evaluation of the experiments presented in **Papers I–III**. Chapter 4 explains the data processing and calculation procedures used to draw conclusions from the experimental findings. Chapter 5 summarizes and discusses a set of important experimental findings. Chapter 6 contains the concluding remarks, as well as recommendations for further research in the fields of steam cracking of plastics in DFB systems.

CHAPTER 2

2 – The Landscape

2.1 Thermochemical recycling principle

Thermochemical recycling involves a set of processes for producing the molecular building blocks of the feedstock.² Such recycling processes, when applied to plastic waste, allow, in theory, unlimited recycling of any plastic material. Thermochemical recycling of plastics comprises three complementary recycling routes,² as depicted in Figure 2.

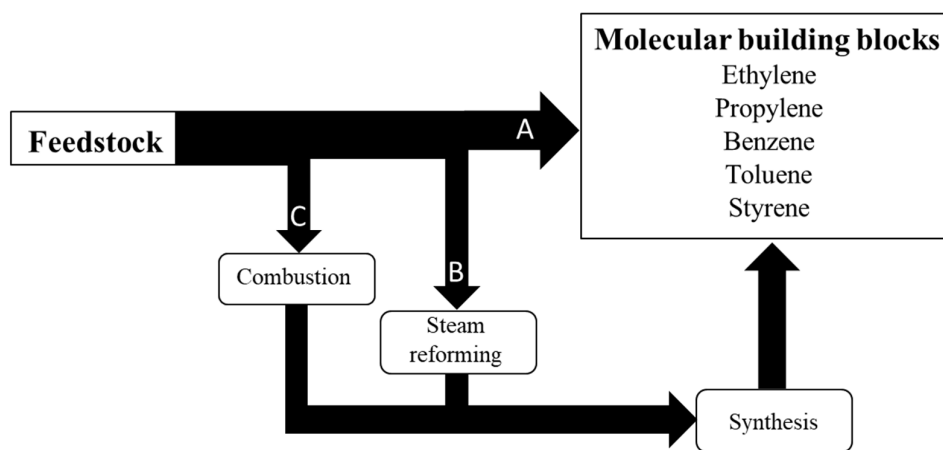


Figure 2. The three recycling routes involved in the thermochemical recycling of plastics.

In this system, Route A is based on the direct production of the molecular building blocks from the feedstock. During conversion through Route A, part of the feedstock ends up as byproducts that are not suitable for plastic production. In this sense, Routes B and C represent the indirect production of the molecular building blocks from the byproducts obtained through Route A. The indirect production of the molecular building blocks corresponds to a combination of combustion, reforming and synthesis processes.

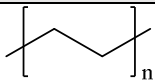
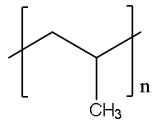
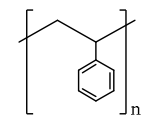
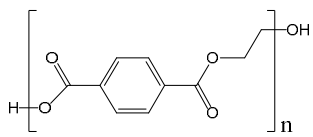
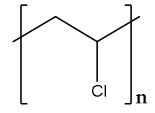
In particular, Route B involves steam reforming of the byproducts (e.g., CH₄) of Route A, and subsequent adjustment of the H₂/CO ratio of the syngas to allow downstream production of the molecular building blocks. The indirect production of the molecular building blocks can be implemented, for instance, via methanol, whereby methanol is converted to olefins through the Methanol-to-Olefins (MTO) process.^{17,18} An important aspect to consider for the implementation of the synthesis processes is the (H₂ – CO₂)/(CO + CO₂) ratio of the syngas, which is commonly referred to as the ‘R ratio’. Conventional synthesis processes require an R ratio of 2.^{19,20} The R ratio of a syngas can be increased by the addition of pure H₂ to the gaseous mixture.^{19,20}

Route C refers to the combustion of those products that are not suitable for use in Routes A and B. This is followed by the recovery of the carbon atoms in the form of CO₂. The recovered CO₂ can be forwarded to synthesis processes downstream,²¹ to avoid any leakage of carbon atoms from the system. Synthesis of the molecular building blocks through Route C also requires an additional input of pure H₂ to the system, which can be fulfilled, for instance, by the electrolysis of water.²¹ Route B and/or Route C must be applied in combination with Route A to achieve 100% carbon recovery of the feedstock.

If the aim is to produce the same type of plastic as the original, Route A is preferable from a thermodynamic point-of-view because the molecular structure of the feedstock is preserved during conversion. The production of molecular building blocks via Route A is dependent upon the molecular composition of the feedstock. This route corresponds to the naphtha/alkane steam cracking process, which is currently used for the production of the molecular building blocks at an industrial scale. Therefore, feedstocks that have naphtha-like molecular structures are suitable for producing the molecular building blocks through Route A. In contrast, the production of the molecular building blocks through Routes B and C is less feedstock-dependent and offers feedstock flexibility to the recycling system. Table 1 summarizes the thermochemical conversion products of the most common types of plastics found in the waste streams.

Polyolefins, which include polyethylene (PE) and polypropylene (PP), have a molecular structure similar to that of naphtha. Research conducted over the last few decades has established polyolefins as promising feedstocks for the production of the molecular building blocks, such as ethylene and propylene, using the steam cracking process.^{2,6,7} However, in reality, the waste streams available for thermochemical recycling will comprise a heterogeneous mixture of different materials and polyolefins. Currently, polyolefins account for more than 50% of all the plastic materials in the waste stream.³ Nevertheless, this fraction can be separated, to some extent, from the other fractions [e.g., polyvinyl chloride (PVC), polystyrene (PS), cardboard, paper, etc.], without the need for advanced sorting techniques. Therefore, thermochemical recycling facilities that are dedicated to the steam cracking of polyolefin-rich plastic wastes have the potential to achieve a circular economy for plastics. **Papers I–III** focus on the steam cracking of feedstocks that have molecular structures similar to that of petroleum naphtha.

Table 1. Thermochemical recycling products of the most common type of plastics found in plastic waste streams.

Plastic type	Molecular structure	Thermochemical process	Major products
Polyethylene (PE)		Steam cracking (700–800°C)	Light olefins (40%-60%), mono
Polypropylene (PP)		Pyrolysis (500–700°C)	aromatics (10%-20%), aliphatic hydrocarbons (C ₆ – C ₃₀) ^{2,6,7,22}
Polystyrene (PS)		Pyrolysis (515°C)	Styrene (72%) ⁶
Polyethylene terephthalate (PET)		Steam gasification (750–800°C)	CO (10%–20%), CO ₂ (35%–65%), benzene (10%–20%) ²³
Polyvinyl chloride (PVC)		Pyrolysis (520°C)	HCl (56%), solid carbon (9%) ²⁴

2.2 Steam cracking

Steam cracking is a process in which saturated hydrocarbons are broken down into smaller, often unsaturated hydrocarbons in the presence of a steam environment.⁹ It is the principal method for producing the molecular building blocks used in the plastic industry. In the industrial steam cracking process, a gaseous (LPG) or liquid (petroleum naphtha) feedstock is diluted with steam, and then briefly heated in a furnace in the absence of oxygen.⁹ Given the structural similarities of naphtha and polyolefins, the products of polyolefin steam cracking are comparable to those of naphtha cracking.

2.2.1 Feedstocks with the polyolefin-type molecular structure

Waste streams that are rich in polyolefins, such as PE and PP, represent the most-suitable feedstock for the recycling system (Figure 2). However, the recycling system, when restricted to using a polyolefin-rich waste stream, will always require additional feedstocks that have a similar molecular structure, to meet the ever-increasing demand for different plastic materials.

In this context, vegetable oils that have naphtha-like paraffinic chains^{25,26} represent a suitable feedstock for producing the molecular building blocks using the steam cracking process. Vegetable oils are composed of complex mixtures of fatty acids (FA). These FA are carboxylic acid molecules with a long aliphatic chain that can be either saturated or unsaturated. The aliphatic chains present in vegetable oil molecules are analogous to the molecules of polyethylene. In vegetable oils, these FA are in the form of triglycerides, i.e., three fatty acid molecules connected to a glycerol backbone through the carboxyl group.^{25,26} Figure 3 shows the molecular structure of rapeseed oil, which is one of the most widely used vegetable oils for cooking purposes.²⁷ Unsaturated fatty acids (USFA), such as oleic acid, linoleic acid, and linolenic acid, account for up to 92% of the total FA content of rapeseed oil, while the remainder (8%) comprises saturated fatty acids (SFA). The SFA and USFA contents of vegetable oil depend on the type of vegetable oil (palm oil, sunflower oil, cottonseed oil, etc.). Nonetheless, the basic structure of the triglyceride molecules remains the same, except for changes in the numbers and positions of the carbon-to-carbon double bonds.²⁸

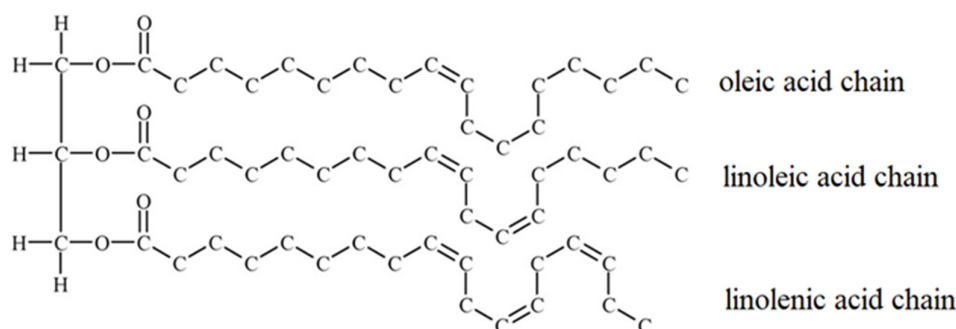


Figure 3. Molecular structure of rapeseed oil.

Apart from their suitability for steam cracking, vegetable oils represent a significant fraction of the available biogenic carbon resources. Global production of vegetable oils reached 210 MMT in Year 2020,²⁹ with about 17 MMT of this ending up in waste streams as waste cooking oil (WCO).^{30,31} The global production level of WCO represents a valuable feedstock for the plastic industry, considering the 11.2 MMT/year increase in the demand for plastic materials. Therefore, the carbon deficit in the plastic recycling system can be compensated almost entirely by adding WCO as a feedstock to the system.

Most of the research studies on WCO valorization conducted to date have focused on energy recovery, either through direct incineration or through synthesizing biofuels.³²⁻³⁶ This has led to the widespread adaptation of WCO as a feedstock for biofuel production at industrial scale. The hydrocracking process is widely used for the production of hydrogenated vegetable oil, commonly referred to as HVO diesel.³⁷ Concomitant with HVO diesel production, propane and hydrocarbons in the range of naphtha and kerosene are obtained as byproducts from the hydrocracking of vegetable oils.^{38,39} Figure 4 depicts the typical product distribution obtained from the hydrocracking of vegetable oils, based on data from the literature.^{38,39} Two of the abovementioned products, naphtha and propane, are suitable feedstocks for the steam cracking process to produce the molecular building blocks. Although the hydrocracking process

represents an important opportunity for bio-based chemicals, it has been commercialized mainly for the production of transportation fuel.

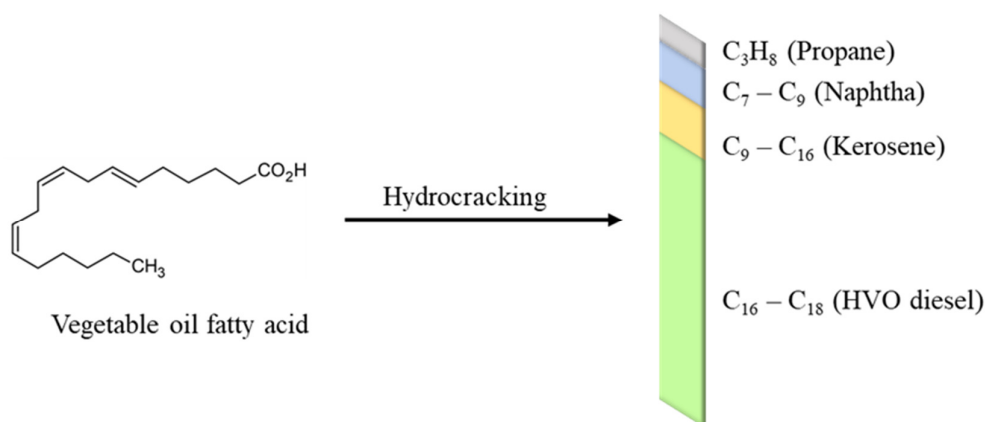


Figure 4. Typical product distribution from the hydrocracking of vegetable oil. (The sizes of the colored bars are proportional to the yields of the respective products).

At the outset of this work, the literature on the direct production of the molecular building blocks from WCO or vegetable oils was scarce. A database with experimental results supporting the suitability of WCO or vegetable oils to produce the molecular building blocks is essential for the development of such recycling technologies. The suitability of WCO for the steam cracking process is evaluated in **Paper III**, which aims to define the direct yields of the molecular building blocks from the fatty acids present in rapeseed oil.

2.2.2 Reactions governing the steam cracking of polyolefins

The products obtained from the steam cracking of polyolefins can be categorized into three different groups based on their physical state under normal conditions:

1. Gas: H_2 , CO , CO_2 , $C_1 - C_5$ hydrocarbons.
2. Liquid: $C_6 - C_{30}$ hydrocarbons.
3. Solid: Waxes (C_{30+} hydrocarbons), polycyclic aromatic hydrocarbons (PAHs), solid carbon.

The distribution of the products among these groups is determined by the cracking conditions, which are commonly referred to as the ‘cracking severity’. Cracking severity indicates the extent to which C-C bonds are broken. Cracking at low severity produces gasoline and diesel-range hydrocarbons ($C_6 - C_{30}$). A higher severity is desired when the process is aimed at producing gaseous olefins ($C_2 - C_4$) and mono-aromatic (BTXS) compounds. Increasing the severity leads to steam reforming of the produced hydrocarbon species.⁷ In industrial cracking processes, the cracking severity is usually associated with the reaction temperature: the higher the temperature, the higher the cracking severity.⁹ The evolution of the steam cracking products of polyolefins with respect to the cracking severity is depicted in Figure 5.

Steam cracking of polyolefins is known to proceed through a free radical type of reaction mechanism.¹⁴⁻¹⁶ The initial polyolefin molecules undergo C-C bond scission to produce free radical species. These free radical species are stabilized by means of hydrogen transfer reactions.¹⁴⁻¹⁶ The transfer of hydrogen atoms occurs among the different radical species, in a reaction that is referred to as ‘intermolecular hydrogen transfer’. Intermolecular hydrogen transfer also occurs between a stable molecule and a free radical species. Furthermore, the transfer of hydrogen atoms that happens within a free radical is known as ‘intramolecular hydrogen transfer’. Intramolecular and intermolecular hydrogen transfer reactions result in C-H bond scission. New free radicals and hydrocarbons with different H/C ratios are produced as the C-C and C-H bond scissions propagate.¹⁴⁻¹⁶ The C-C and C-H bond scissions propagate until all the free radicals are stabilized.¹⁴⁻¹⁶ Intermolecular and intramolecular hydrogen transfer reactions are described in Figure 6.

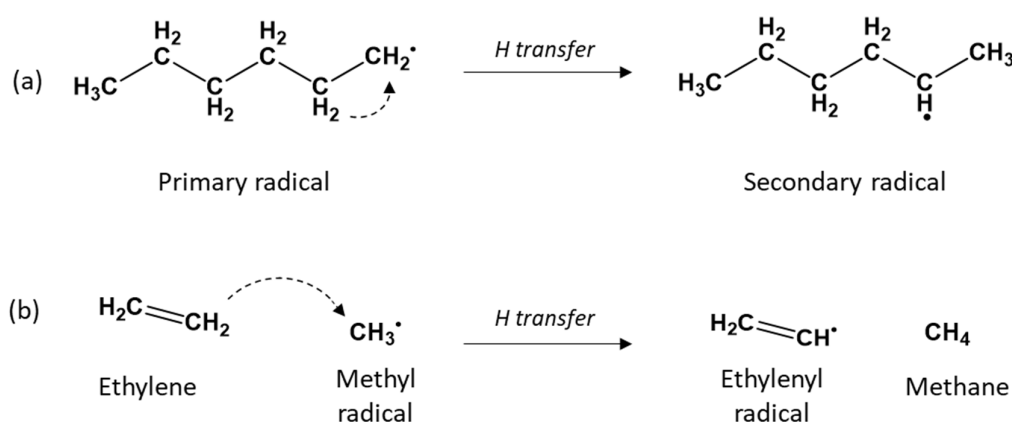


Figure 6. (a) Intramolecular hydrogen transfer; (b) Intermolecular hydrogen transfer.

The products obtained from the steam cracking of polyolefins can be further divided into three groups based on their hydrogen-to-carbon (H/C) ratios:

1. $\text{H/C} < 2$: di-olefins, tri-olefins, aromatics, carbon oxides, solid carbon.
2. $\text{H/C} = 2$: mono-olefins.
3. $\text{H/C} > 2$: paraffins.

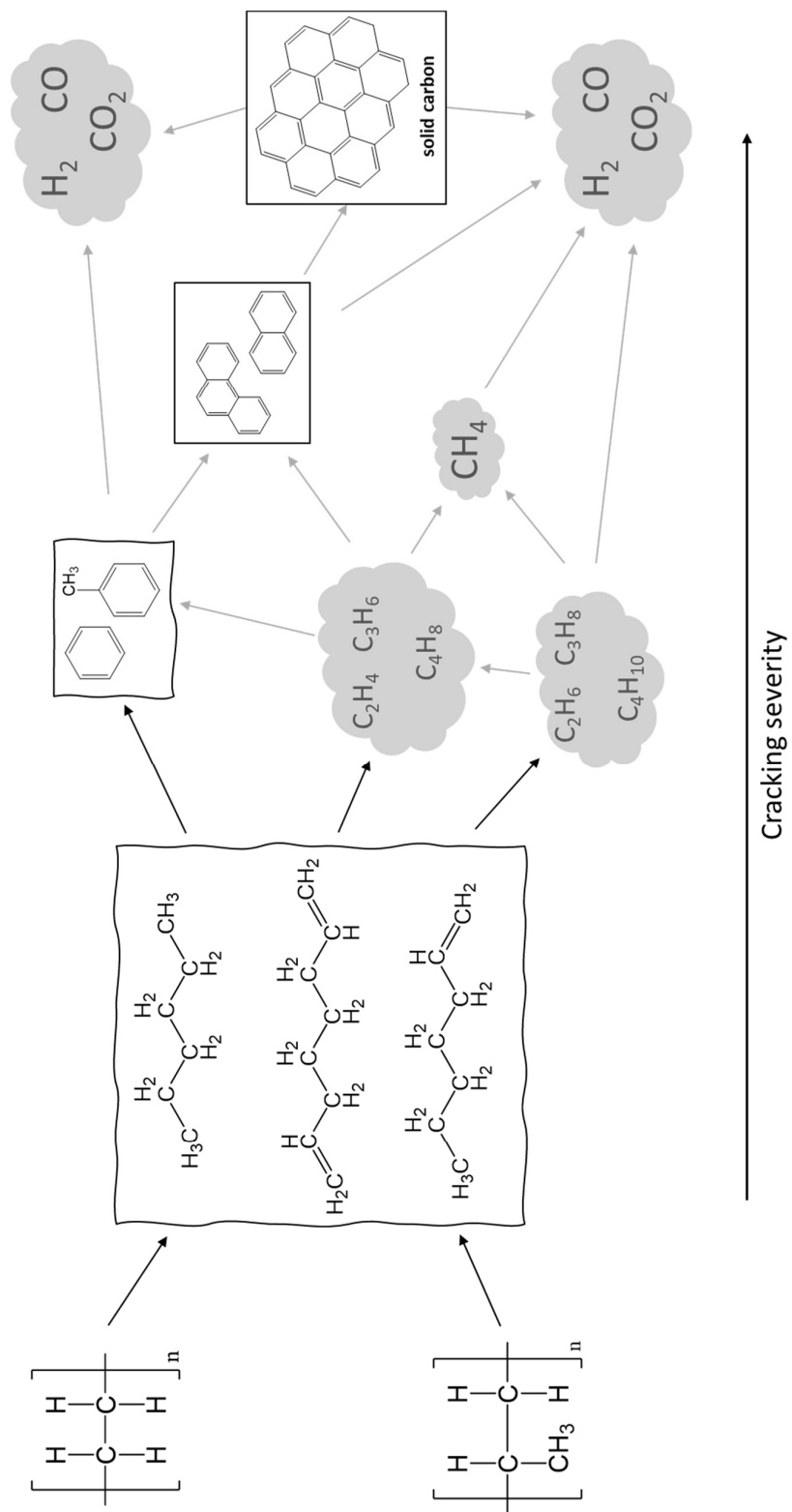


Figure 5. Evolution of the steam cracking products with respect to the cracking severity.

Irrespective of the cracking severity, the products of steam cracking will always fall into the abovementioned three groups. The distribution of the products among these groups is governed by the propagation of C-H bond scission. The extent to which C-H bond scission propagates is referred to as the ‘hydrogen transfer severity’, which here is defined as the extent to which the average H/C ratio of the steam cracking products deviates from the H/C ratio of the feedstock. **Papers I and II** reveal the influence of the hydrogen transfer severity on the distribution of products obtained from the steam cracking of PE among the abovementioned three groups. The evolution of the steam cracking products with respect to hydrogen transfer severity is described in Figure 7.

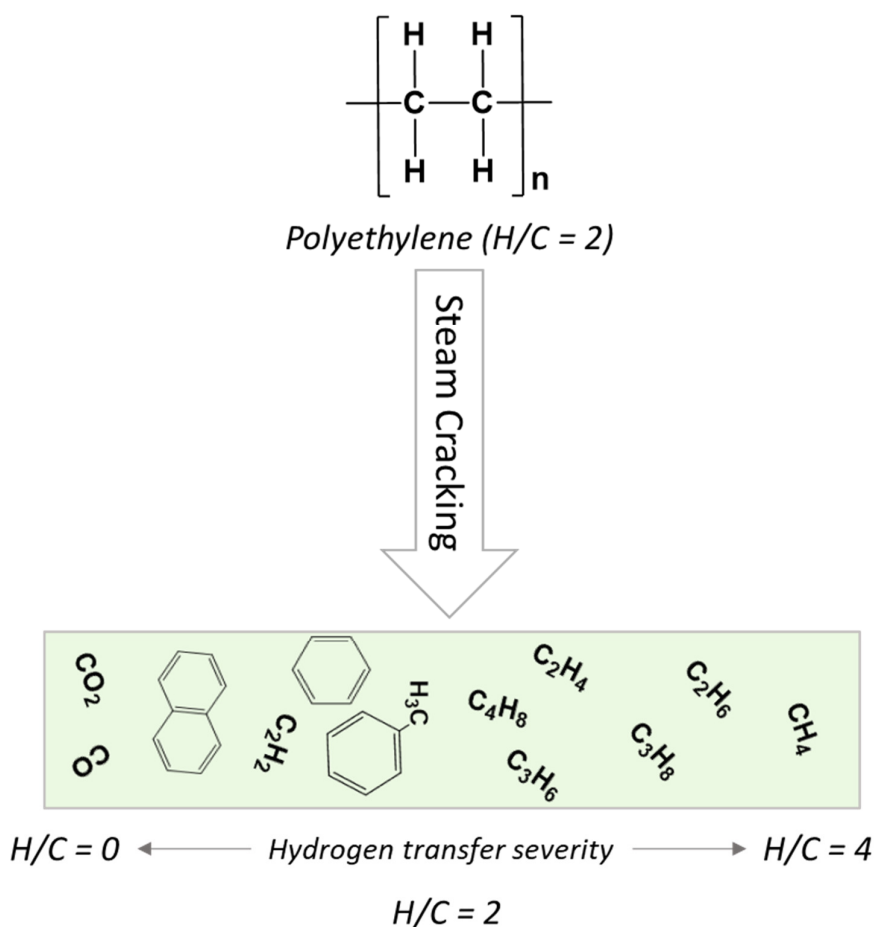
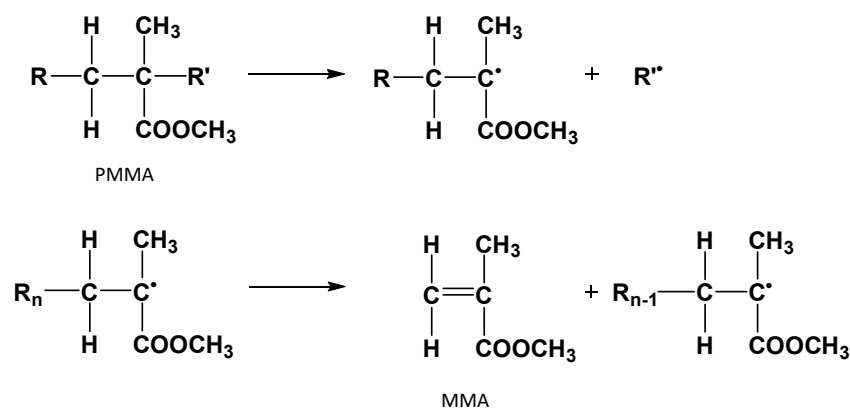


Figure 7. Evolution of the steam cracking products of polyethylene as a function of hydrogen transfer severity for a certain cracking severity.

In the absence of hydrogen transfer reactions or C-H bond scission, the cracking of a hydrocarbon molecule would give products with the same H/C ratios as that of the feedstock. For example, cracking of polymethyl methacrylate (PMMA) and PS gives a yield of 97 wt.% and 72 wt.% of their monomers, methyl methacrylate and styrene, respectively.^{6,40} The steric hindrance caused by the presence of bulky functional groups, such as -COOCH₃ and -C₆H₅, along the polymeric chains of PMMA and PS, respectively, hinders the intermolecular and intramolecular hydrogen transfer reactions. The cracking of PMMA is described by Equation 1.



Equation 1

Unlike PS and PMMA, polyolefins such as PE and PP do not contain bulky functional groups along their polymer chains. The lack of steric hindrance along the polymeric chains of PE and PP promotes the hydrogen transfer reactions among the free radicals during steam cracking (see Figure 6a). Therefore, the cracking severity and the hydrogen transfer severity govern the product distribution obtained from the steam cracking of polyolefins.

2.3 Steam cracking in the DFB reactor configuration

As discussed in *Chapter 1* of this work, the fluidized bed reactor is suitable for the steam cracking of waste plastics due to its heat transfer properties and its ability to handle heterogeneous feedstocks. The DFB reactor configuration, in particular, enables continuous removal of the solid carbon deposits formed during the steam cracking process. In addition, the regenerator reactor of the DFB system (see Figure 1) is an elegant way of providing the heat required for the steam cracking process. That heat can be generated by combusting the solid carbon deposits and/or additional fuel in the regenerator.

The most common industrial cracking process operated with the DFB reactor configuration is the FCC process. In the FCC process, high-molecular-weight hydrocarbon fractions of crude oil are cracked into lighter hydrocarbons in the presence of steam and a catalytically active bed material.⁹ The catalytically active bed materials used in the commercial FCC process consist of microporous aluminosilicates (e.g., zeolites), which act as active sites for the cracking reactions.^{9,41} Many studies on the cracking of polyolefins in the FCC environment have been reported in the literature.⁴²⁻⁴⁶ The use of FCC catalysts as bed materials has been shown to increase the cracking severity of the process, as compared to non-catalytic bed materials, at a given temperature, by lowering the activation energy of C-C bond breakage.⁴²⁻⁴⁶ Activation of the C-C bond is attributed to the presence of catalytically active sites in the bed material. During the FCC process, these active sites undergo deactivation due to irreversible adsorption of feedstock impurities and the formation of solid carbon deposits on the bed material.⁴¹ As a consequence, to sustain the cracking reaction, part of the bed material inventory needs to be replaced with fresh bed material.⁴¹ Despite the capability to activate the C-C bond, the

susceptibility of the FCC catalysts to feedstock impurities makes the commercial FCC process unfavorable for the cracking of heterogeneous plastic waste streams.

Alternatively, a DFB reactor configuration dedicated to the steam cracking of plastic waste streams can be operated with bed materials that are resistant to feedstock impurities (e.g., quartz sand, olivine, etc.).⁴⁷ Steam cracking of high-density polyethylene (HDPE) has been successfully demonstrated in the 2–4-MWth DFB system at Chalmers University of Technology, Gothenburg.² Thunman et al. have shown that products derived from the steam cracking of HDPE in the 2–4-MWth Chalmers DFB system are comparable to the typical product distribution obtained from a tubular naphtha cracker.² Wilk and Hofbauer have also investigated the formation of monomers and aromatic hydrocarbon species during the steam cracking of different polyolefin materials in a 100-kW DFB system.⁷ Natural ores, silica sand and olivine were used as the bed materials in the DFB steam cracking process by Thunman et al.² and Wilk et al.⁷, respectively. Compared to the FCC catalysts, some natural ores are known to have lower catalytic activities towards the breakage of the C-C bond.⁴⁸ However, the influences of such bed materials on C-H bond breakage or the hydrogen transfer severity in fluidized bed steam cracking processes remains unknown.

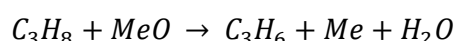
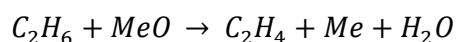
Paper I reveals the effect that the bed material has on the hydrogen transfer severity of the PE steam cracking process. In particular, the influence of the transition metal content of the bed material on C-H bond breakage is demonstrated. Transition metal-containing bed materials have been widely exploited in DFB processes, such as Chemical Looping Combustion (CLC), Chemical Looping Gasification (CLG) and Chemical Looping Oxidative Dehydrogenation (CL-OHD), for the conversion of carbonaceous materials.^{49–51} Nevertheless, the impacts of bed materials that contain transition metals on the steam cracking of polyolefins remained unexplored at the inception of this work.

When DFB systems are operated with bed materials that contain transition metals oxygen transfer occurs between the two reactors, without exchange of any other gas. This phenomenon is known as ‘oxygen transport in DFB’. The transition metals in a DFB system undergo a continuous cycle of oxidation and reduction. The transition metals are oxidized in the presence of air in the regenerator and are reduced in the presence of hydrocarbons and syngas in the cracker or the thermochemical reactor. Thus, oxygen transport stimulates an oxidizing environment in the thermochemical reactor, inevitably oxidizing, either partially or completely, the feedstock in the thermochemical reactor.

As mentioned earlier, the steam cracking of polyolefins is primarily aimed towards the production of petrochemical feedstocks, such as olefins, paraffins, aromatics and pyrolysis oil. The oxidation of the feedstock during the cracking process is, therefore, considered undesirable because it reduces the direct production of the abovementioned economically valuable hydrocarbons. DFB cracking processes, such as the FCC process, are unlikely to experience oxidation of the feedstock by the bed material in the cracking reactor. This is because such processes deal with relatively pure hydrocarbon feedstocks and tailored catalytic bed materials. On the other hand, the development of oxygen transfer in DFB systems that are dedicated to the steam cracking of plastic waste, is in most cases unavoidable due to the inherent properties of the natural ores used as the bed materials. Apart from the inherent properties of the bed material, the ash fraction of the feed used in DFB systems also contributes to oxygen transfer

through ash particles that are mixed with the bed material or by the formation of an ash layer on the bed material particles.⁴⁹

The influences of transition metal oxides on C-H bond breakage are well-established for the CL-OHD process. The CL-OHD process has been used for the dehydrogenation of ethane and propane for the production of ethylene and propylene, respectively, by means of a transition metal oxide.⁵⁰ CL-OHD of ethane and propane takes place through the redox reactions described in Equation 2.



Equation 2

In the CL-OHD process, the oxygen transport effect of the bed material dehydrogenates the paraffin molecules through dissociation of the C-H bonds.⁵⁰ Furthermore, in terms of the CLG process, the transition metal content of the bed material is linked to the extent to which carbon is converted to CO₂ in the gasifier.⁴⁹ Pissot et al. have described the product distribution derived from CLG of automotive shredder residue (ASR) in the 2–4-MWth Chalmers DFB gasifier, and they have demonstrated the development of oxygen transport properties by the bed material as a result of the high metal content of the ASR.⁴⁹ Based on these findings, the hydrogen transfer severity of steam cracking is expected to increase in the presence of a bed material that contains transition metals. In particular, the steam cracking products of polyolefins are expected to have an average H/C ratio of <2.

The increase in hydrogen transfer severity is regarded as undesirable because it lowers the direct production of the molecular building blocks with H/C ratios of 2 (e.g., ethylene, propylene and butadiene). Moreover, the increase in the hydrogen transfer severity increases the production levels of methane, carbon oxides and PAHs (see Figure 7). The valorization of these compounds to the molecular building blocks through Routes B and C (Figure 2) incurs an increased thermodynamic penalty for the overall recycling system. For the polyolefin recycling system (Figure 2) to incur the minimum thermodynamic penalty, the hydrogen transfer severity of the steam cracking step (Route A) should be as low as possible.

The enhanced formation of the molecular building blocks (H/C ratio of 2), concomitant to the suppression of hydrogen transfer severity, can be ensured by hydrogenating the unstable free radical species. As mentioned earlier, the propagation of C-H bond scission ceases once all the free radical species have been stabilized. The hydrogenation reaction of ethylenyl, an unstable free radical, is described by Equation 3.



Equation 3

The thermochemical process that involves simultaneous cracking and hydrogenation of hydrocarbons is commonly referred to as the ‘hydrocracking process’.⁵² The hydrocracking

process involves the cracking of hydrocarbons, followed by hydrogenation of the cracked hydrocarbons by reactive hydrogen to produce stable and lighter hydrocarbons.⁵² Hydrogenation of the free radicals produced during hydrocarbon cracking prevents intermolecular H atom transfer, thereby reducing the hydrogen transfer severity of the cracking process. In addition, hydrocracking facilitates the production of compounds with higher H/C ratios than the feedstock.⁵² The hydrocracking process is commonly used to convert heavy petroleum products into lighter chemicals in the presence of a catalyst and a hydrogen atmosphere.⁵² Hydrocracking of plastic materials, in particular polyolefins, has also been studied extensively in recent years.⁵³ The reduced formation of aromatics and solid carbon makes the hydrocracking process more-favorable than other processes such as steam cracking and pyrolysis.⁵⁴ In addition, the presence of hydrogen enables the removal of heteroatoms such as chlorine, which may be present in plastic waste streams.⁵³

An alternative to hydrocracking in a hydrogen atmosphere is hydrocracking with hydrogen donors, which has been extensively studied in the past.⁵⁵⁻⁵⁸ The hydrogen released by the hydrogen-donors stabilizes the free radicals produced during the cracking reactions, as described in Equation 3. The hydrogen-donation capabilities of cyclic hydrocarbons such as cyclohexane and decalin have been extensively reported on in the literature.^{55,56} Furthermore, the hydrogen-donation capability of water molecules in a supercritical steam environment has also been explored with regard to upgrading heavy crude oil products.⁵⁹⁻⁶² Supercritical water, being a hydrogen donor, has been shown to increase the H/C ratios of the products, as compared to that of the feedstock, by transferring its hydrogen atoms to the free radicals. The transfer of hydrogen atoms happens on the surface of a transition metal oxide catalyst and is attributed to the redox potential and the water dissociation capability of the metal oxide catalyst.⁶⁰⁻⁶³

The abovementioned hydrocracking processes usually require a catalyst that facilitates the hydrogenation of the free radicals. The catalyst enables the transfer of hydrogen from the surroundings to the hydrocarbon species.⁵² In the absence of the catalytically active transfer sites, hydrogen is released as H₂ into the surroundings, which means that it is not available to contribute to the hydrogenation reaction. Therefore, the hydrogenation of the free radicals during hydrocracking not only depends on the hydrogen-donation capability of the surrounding species, but also on the hydrogen-transfer capability of the catalyst.⁵²

The presence of a bed material that contains transition metals and of a steam-rich environment in a fluidized bed steam cracking process provides an opportunity to explore the hydrocracking capability of such a process. In particular, a DFB can be a suitable reactor system for hydrocracking through hydrogenation by steam due to its ability to circulate the bed material through continuous redox cycles. Hydrocracking through hydrogenation by steam was investigated in **Paper II**. At the inception of this work, there were no previous studies reporting hydrogenation by water molecules in the fluidized bed steam cracking process. **Paper II** elucidates the hydrogen-donation capability of water molecules on the surface of the fluidized bed material, which increases the share of valuable hydrocarbons (H/C = 2) among the products of steam cracking. The investigation looks at two aspects: (1) the ability of the bed material to undergo redox cycles and generate H₂ via the water dissociation reaction; and (2) the transfer of hydrogen, generated by the water dissociation reaction, to the steam cracking products.

CHAPTER 3

3 – Experimental Setup

The steam cracking experiments described in this work were performed in a laboratory-scale bubbling fluidized bed (BFB) reactor. The BFB reactor used in this work resembles the cracking reactor of a DFB steam cracker. In this chapter, the experimental facility is described, as well as the product gas sampling and analytic methods. The determination of the overall carbon balance closure of the steam cracking process is explained. Also described are the compositions of the bed materials and feedstocks used in the different experiments.

3.1 Description of the BFB steam cracker

The reactor setup used in this work is shown in Figure 8. The BFB steam cracker is a stainless-steel tube with a height of 1.305 m and an internal diameter of 88.9 mm. The reactor is heated externally with an electric furnace. The temperature along the height of the reactor is measured and logged continuously by thermocouples placed inside the reactor. The bed material is loaded at the top of the reactor before heating the reactor. The temperature of the bed material is measured by the bottom-most thermocouple (see Figure 8) and is considered the reaction temperature. The temperature in the freeboard is measured by the other two thermocouples.

The gases required for fluidizing the bed material are introduced separately and mixed homogeneously in a windbox before entering the reactor through a gas distributor plate. The volumetric flow of the fluidization gases is controlled by mass flow controllers (MFCs). A split stream of the gases leaving the reactor can be sampled through one of the gas sampling ports: h1 to h3 (Figure 8).

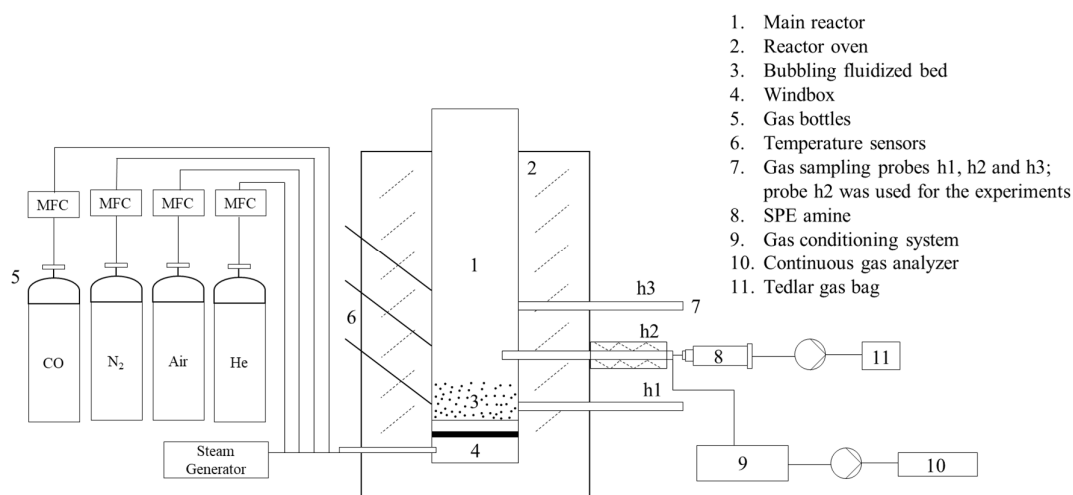


Figure 8. Schematic of the experimental setup.

A gas sampling probe is inserted into the reactor through one of the ports, while the remaining ports are closed to prevent the bed material from entering the port. The height of the port is selected depending on the height of the fluidized bed. The probe is heated to 350°C with an electrical heating band, to avoid condensation of hydrocarbons and steam. The sampled gas is then divided into two split streams: one stream is passed through a gas conditioning system, while the other stream is passed through a solid-phase extraction (SPE) amine column.

The gas conditioning system involves scrubbing of the sampled gas with isopropanol, followed by drying with glass wool and silica gel. The cold and dry gas is analyzed in the SICK GMS 820 permanent gas analyzer (SICK AG, Waldkirch, Germany). The SPE amine used is the Supelclean ENVI-Carb/NH₂ tube (Sigma-Aldrich Inc., St. Louis, MO). The gas sampled through the SPE amine is collected in a 0.5-L Tedlar gas bag.

3.2 Feedstocks and bed materials

PE pellets were used as the feedstock for the work presented in **Papers I and II**, and raw rapeseed oil was used as the feedstock for the investigation described in **Paper III**. The PE pellets, with a bulk density of 945 kg/m³ and an average pellet size of 2.5 mm, were provided by Borealis AB (Stenungsund, Sweden). The carbon and hydrogen contents of the PE pellets were calculated based on the PE molecular structure of $-\text{[CH}_2\text{]}-$ repeating units (Table 2). The rapeseed oil used in this work was obtained from a local supermarket in Gothenburg, Sweden. The elemental composition of the rapeseed oil, as presented in Table 2, was calculated based on the average FA composition of rapeseed oil listed in the literature.^{64–67}

Table 2. Elemental compositions of PE pellets and rapeseed oil.

	PE pellets	Rapeseed oil
	(%w/w)	(%w/w)
Carbon (C)	85.70	79.60
Hydrogen (H)	14.20	11.40
Oxygen (O)	0.00	8.97
Sulfur (S)	0.00	0.03

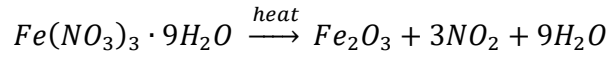
Seven different bed materials were tested in this thesis; Al_2O_3 ; $1\text{Fe}/\text{Al}_2\text{O}_3$; $2\text{Fe}/\text{Al}_2\text{O}_3$; $5\text{Fe}/\text{Al}_2\text{O}_3$; bauxite; olivine; and silica sand. The chemical compositions of the bed materials are listed in Table 3. Of the seven bed materials used in this work, bauxite, olivine, and silica sand were obtained from natural ores. The other four bed materials were synthesized in the laboratory. The elemental compositions of the natural ores (Table 3) were provided by the supplier. The elemental compositions of the synthetic bed materials were calculated based on the synthesis process.

Table 3. Chemical compositions (%wt.) of the tested bed materials.

	Al_2O_3	$1\text{Fe}/\text{Al}_2\text{O}_3$	$2\text{Fe}/\text{Al}_2\text{O}_3$	$5\text{Fe}/\text{Al}_2\text{O}_3$	Bauxite	Olivine	Silica sand
Al_2O_3	99.50	97.20	94.50	86.90	78	0.46	0.17
SiO_2	0.00	0.00	0.00	0.00	15	41.7 ^a	99.2
Fe_2O_3	<0.03	2.80	5.50	13.10	1.3	7.4 ^a	0.054
MgO	0.00	0.00	0.00	0.00	0.2	49.6 ^a	0.00

^aAssumed to be present as silicates of magnesium and iron.

The bed materials used in **Paper I** were tailored in order to determine the exclusive impacts of transition metal oxides on the hydrogen transfer reactions. Fe_2O_3 was selected as a model transition metal oxide. The bed materials comprised Al_2O_3 impregnated with Fe_2O_3 at three different concentrations. Al_2O_3 without iron oxide was used as the reference material. The bed material Al_2O_3 (neutral Al_2O_3 , pH 7 in water) with a purity of 99.5%wt. was obtained from Sigma-Aldrich. The bed materials $1\text{Fe}/\text{Al}_2\text{O}_3$, $2\text{Fe}/\text{Al}_2\text{O}_3$ and $5\text{Fe}/\text{Al}_2\text{O}_3$ were synthesized by incipient wetness impregnation of iron (III) nitrate nonahydrate ($\text{Fe}(\text{NO}_3)_3 \cdot 9\text{H}_2\text{O}$) on Al_2O_3 . Iron (III) nitrate nonahydrate with a purity of >98% was obtained from Fisher Scientific. Bed materials impregnated with iron nitrate nonahydrate were dried overnight in an oven at 105°C, followed by calcination at 700°C in the BFB reactor. Thus, Fe_2O_3 was formed on the surface of the support, according to the following reaction:



Equation 4

The three bed materials that were impregnated with iron oxide had Fe contents (%wt.) of 1%, 2% and 5%, and were, therefore, referred to as 1Fe/Al₂O₃, 2Fe/Al₂O₃ and 5Fe/Al₂O₃, respectively. The synthesized bed materials were investigated using scanning electron microscopy (FEI ESEM Quanta 200), and energy-dispersive x-ray spectroscopy (SEM-EDS) was conducted to evaluate the elemental composition. The bed material particles were fixated with epoxy resin and cross-sections were prepared by grinding with silicon carbide sandpaper before the analysis.

Bauxite and olivine were used in **Paper II** to determine the hydrogen transfer capabilities of the natural ores. The redox potentials of bauxite and olivine were employed to drive the water dissociation reaction required for the hydrogen transfer reactions. Silica sand was used as the bed material for the experiments performed in **Paper III**. The influence of silica sand on the hydrogen transfer reactions was not investigated in this work.

3.3 Chemical looping tests

Chemical looping tests were performed to measure the oxygen transport capacities of the synthetically prepared bed materials: 1Fe/Al₂O₃; 2Fe/Al₂O₃; and 5Fe/Al₂O₃. The oxygen transport capacities of the bed materials were used as indicators of the appropriate impregnation of iron oxide on Al₂O₃.

The chemical looping tests were performed in the BFB reactor described previously. The bed materials were subjected to a cyclic process of reduction and oxidation for four cycles, to measure their oxygen transport capacities. A gas mixture of N₂ and CO was used as the fluidization medium during the reduction stage, followed by air during the oxidation stage. The chemical looping tests were performed at a bed material temperature of 700°C. The experimental conditions for the chemical looping tests are detailed in Table 4. A part of the fluidization gases leaving the reactor was sampled through port h2 (see Figure 8) and analyzed continuously in the SICK GMS820 permanent gas analyzer. The oxygen transport capacity of each bed material was calculated according to the following equation:

$$\text{oxygen transport capacity, \%w} = \frac{M_o}{M_b} \times 100$$

Equation 5

In Equation 5, M_o is the mass of oxygen released by the bed material as CO₂, and M_b is the total initial mass of the bed material. M_o is calculated from the fraction of CO that is converted to CO₂ by the bed material during the reduction phase. The fraction of CO converted to CO₂ was determined from the concentration profile of CO₂ logged by the permanent gas analyzer, during the reduction phase.

Table 4. Experimental conditions used for the chemical looping tests.

Stage	Temperature (°C)	Duration (min)	Gas flow rate
Reduction	700	2	4.0 l _N /min, 25% vol. CO/N ₂
Inert	700	1	3.0 l _N /min, 100% N ₂
Oxidation	700	3	4.0 l _N /min, Air

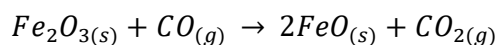
3.4 Blank water dissociation test

The abilities of bauxite and olivine to undergo redox cycles and generate hydrogen were determined by performing a blank water dissociation test and quantifying the amount of hydrogen generated by the bed materials. The blank test was performed at a bed material temperature of 750°C. The procedure for the blank water dissociation test is described in Table 5.

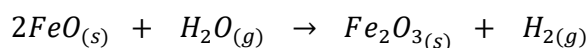
Table 5. Experimental procedure for the blank water dissociation test.

Experimental stage	Fluidization gases (l _N /min)			Time
	N ₂	Steam	CO	
Reduction	2.0	0.0	3.0	180 s
Inert	2.0	0.0	0.0	Until 0 %vol CO
Hydrogen generation	2.0	4.0	0.0	Until 0 %vol H ₂

During the reduction stage, the bed materials were reduced by a mixture of CO and N₂ for a time period of 180 s. The iron oxide content of the bed materials was reduced according to the following equation:

**Equation 6**

The reactor was then purged continuously with N₂ to create an inert atmosphere. After the reactor was rendered inert, the bed material was exposed to steam as one of the fluidization gases. The steam added to the reactor was converted into hydrogen by the bed material according to the following steam-iron reaction:



Equation 7

A part of the gases leaving the reactor during the blank test was sampled and analyzed for composition (%vol) using the continuous gas analyzer. The known volume of N₂ (Table 3) was used to estimate the molar yield of hydrogen, according to the ideal gas law (Equation 8).

$$n_{H_2} = \frac{\%vol_{H_2}}{\%vol_{N_2}} \cdot n_{N_2}$$

Equation 8

In Equation 8, n_{H_2} and n_{N_2} represent the moles of N₂ and H₂, respectively. The terms %vol_{H₂} and %vol_{N₂} indicate the concentrations (%vol) of H₂ and N₂ in the gases leaving the reactor, as measured by the continuous gas analyzer.

3.5 Steam cracking tests

The feedstocks, PE pellets (**Papers I and II**), and rapeseed oil (**Paper III**), weighing 2 g per batch, were fed to the top of the fluidized bed during the steam cracking tests. The steam cracking of PE was performed at 700°C (**Paper I**) or 750°C (**Paper II**). The steam cracking of rapeseed oil was performed at three different temperatures: 650°C, 700°C, and 750°C. The steam cracking temperatures mentioned here correspond to the temperature of the bed material before it came into contact with the feedstock. The experiments performed with rapeseed oil as the feedstock are, hereinafter, referred to as RO650, RO700, and RO750 for the bed material temperatures of 650°C, 700°C, and 750°C, respectively.

The experimental setup used in this work represents a batch-wise steam cracking process. Such a system with a low feed would have significant evaporation losses due to radiative heat transfer from the walls of the reactor. Considering the physical states of the feedstocks, it seems unlikely that evaporation losses from the PE pellets occur before they come in contact with the bed material. However, rapeseed oil, being liquid and volatile, may undergo evaporation before it reaches the surface of the bed material. A reactor setup with continuous feeding is desirable to avoid this problem. To recreate such a feeding system, each batch of rapeseed oil was frozen at -18°C to reduce its surface area to volume ratio, thereby minimizing losses due to evaporation. The steam cracking tests performed in this work followed the procedure described in Table 6.

Table 6. Experimental procedure for the steam cracking tests.

Experimental stage	Fluidization gases (l _N /min)				Time
	N ₂	Steam	Air	He	
Oxidation of the bed material	0.00	0.00	5.00	0.00	Until 20.9 %vol O ₂
Cracking	2.00	4.00	0.00	0.05	120 s (90 s, Paper III)
Carbon deposits combustion	0.00	0.00	5.00	0.05	120 s (90 s, Paper III)

The bed material was exposed to an oxidizing environment at the desired reaction temperature before it came in contact with the feedstock. Oxidation of the bed material was achieved by fluidizing the bed material with air. A part of the gases leaving the reactor was continuously sampled through sampling port h2 (see Figure 8), to monitor the concentration of O₂ in the reactor. Complete oxidation of the bed material was assumed when the O₂ concentration inside the reactor matched the ambient O₂ concentration of 20.9 %vol. The bed material was fully oxidized before each steam cracking test, to simulate the conditions of a DFB cracker (see Figure 1) where the bed material enters the cracking reactor after having been fully oxidized in the regenerator. Helium was used as one of the fluidization gases during the cracking and carbon deposit combustion stages of each experiment. The volumes of the gases produced during carbon deposit combustion and cracking were determined, using helium as a tracer gas.

The steam cracking tests produced three main types of products:

1. Gas: H₂, CH₄, C₂H₄, etc.
2. Liquid: benzene, toluene, other aromatics, etc.
3. Solid: solid carbon deposits.

The gaseous and the liquid products exit the reactor along with the fluidization gases, while the solid carbon deposits remain in the reactor along with the bed material.

A part of the gas sampled during steam cracking was analyzed for its H₂, CO, CO₂ and CH₄ concentrations (%vol). The cracking stage was continuously monitored to determine the total time required to crack the feedstock, as well as to ensure that there were no product gases left after the sampling period.

For a comprehensive analysis of other product species, a slipstream of the sampled gas during the cracking stage was passed through the SPE amine column. Gases leaving the SPE amine were collected in a 0.5 L Tedlar gas bag. The gas samples collected during each experiment were analyzed in the Agilent 490 micro-GC system. The Agilent micro-GC has four different columns, each with a TCD detector. A summary of the gases measured by the micro-GC system is presented in Table 7. The detection of aliphatic compounds with more than five carbon atoms was beyond the scope of the analytic methods used in this work. The uncalibrated CP-WAX column was used to detect benzene and toluene in the collected gas samples.

Table 7. Gases measured by the Agilent 490 micro-GC system.

Column	Gases	Calibration
CP-Cox	He, H ₂ , Air (coelution of N ₂ and O ₂), CO, CH ₄	4-point calibration
PoraPLOT U	CO ₂ , C ₂ H ₄ , C ₂ H ₆ , C ₂ H ₂ , C ₃ H _x	4-point calibration
CP-WAX 52 CB	Benzene, Toluene	No calibration
CP-Sil 5 CB	C ₄ H _x , C ₅ H _x	1-point calibration

The quantification of the liquid or aromatic hydrocarbons was performed with the BRUKER GC-FID system using the solid-phase adsorption (SPA) method described by Israelsson et al.⁶⁸ The redundant measurements of benzene and toluene performed on the CP-WAX column of the micro-GC system were made to ensure that all of the benzene and toluene were captured and quantified by the SPA method. The yield of solid carbon deposits was measured by combustion in the presence of air and measurement of the amounts of CO and CO₂ produced during the process. The fluidization gases were changed from steam and nitrogen to air to allow combustion of the carbon deposits in the bed material. The combustion gases were sampled and collected in a separate 0.5-L Tedlar bag for GC analysis. The compositions of the combustion gases collected in the gas bag were determined using the micro-GC system.

3.6 Hydrocracking tests

As discussed earlier, hydrocracking of PE through hydrogenation by water molecules was the focus of **Paper II**. The hydrogen-donation capability of water molecules was determined by performing the steam cracking tests concurrently with the water dissociation reaction on the surface of the bed material. The water dissociation reaction was driven by employing the redox potentials of bauxite and olivine, which contained iron oxide in reduced form.

Prior to the steam cracking tests, the bed materials were fluidized with a mixture of CO and N₂, to reduce the iron oxides present in the bed materials. The bed materials were fluidized with a CO/N₂ mixture until the concentration of CO₂ exiting the reactor reached 0 %vol. The fluidization gases were then switched to N₂ for 2 min to purge the reactor and create an inert environment. Steam was added to the fluidized bed after the concentration of CO reached 0 %vol.

The PE pellets were dropped directly on the top of the reduced fluidized bed after steam was added to the reactor. This ensured that the steam cracking and water dissociation reactions occurred simultaneously. The procedures for sampling and analysis of the species produced during the steam cracking of PE with concurrent water dissociation were the same as those described in Section 3.5.

CHAPTER 4

4 – Data Processing and Analysis

The experimental results obtained in this thesis were derived from the same sampling, analysis, and evaluation methods as described in this chapter. As a result, the systematic errors for all the data-points are expected to be similar, rendering the observed trends statistically significant. The experimental results reported in the following sections are the average values derived from multiple repetitions of the performed experiments.

The products obtained from the steam cracking experiments performed in this work are divided into different groups based on the sampling and analytic methods used for their quantification. The groups of products applied in this work for the carbon balance calculations are described in Table 8. The micro-GC system used for the quantification of gaseous products detected all C₃, C₄, and C₅ compounds as C₃H_x, C₄H_x, and C₅H_x, respectively. The separation of these compounds into individual olefins and paraffins was outside the scope of the micro-GC analysis. However, from the literature, it is known that the share of paraffins among the C₃, C₄, and C₅ products is negligible, as compared to the corresponding olefins under reaction conditions similar to those used in the present work.⁶⁹⁻⁷¹ Therefore, for simplicity, C₃H_x, C₄H_x and C₅H_x are placed in the Olefins group along with C₂H₄.

The yields of gaseous products represent the average values for 3–4 gas bags, including five chromatographs for each gas bag, which generally have a relative standard deviation of 0.3%–2.0% for all the gaseous species. The yields of aromatic species represent the average of 3–4 SPA samples, involving nine chromatographs for each sample. The relative standard deviation among the repeats of the SPA samples is usually less than 10%, and for the major aromatic species, such as benzene, toluene, styrene and naphthalene, the deviation is less than 5%, since integration errors are less likely to occur for larger peaks.

The molar yields (mol/kg_f) of the gaseous species collected in the Tedlar gas bags were calculated based on the He-tracing method. Equation 9 was used to calculate the molar yields of all the measured gaseous species.

$$n_i = \frac{c_i}{m_f} \cdot \left(\frac{V_{He}}{C_{He}} \right) \cdot \frac{1}{V_m}$$

Equation 9

In Equation 9, n_i denotes the molar yield and c_i is the concentration of gaseous species i . The terms V_{He} and C_{He} represent the volume and concentration of the tracer helium gas, respectively. m_f is the mass of the feedstock for each batch, and V_m is the volume of one mole of an ideal gas at 25°C and 1 atm (24.5 l/mol). The molar yield of each species is then transformed to the corresponding carbon and hydrogen yields based on the total carbon and hydrogen contents of the feedstock (see Table 2).

Table 8. Groups of species applied in this work for the carbon balance calculations.

	Group	Species included
Gaseous products (Tedlar gas bags)	Olefins:	C ₂ H ₄ , C ₃ H _x , C ₄ H _x , C ₅ H _x
	Paraffins:	CH ₄ , C ₂ H ₆
	Carbon oxides:	CO, CO ₂
	Hydrogen:	H ₂
Aromatic products (SPA)	Benzene:	benzene
	1-ring aromatics:	toluene, xylenes (o/p), styrene
	Naphthalene:	naphthalene
	Other aromatics:	indene, 1,2-dihydronaphthalene, 1-methylnaphthalene, 2-methylnaphthalene, biphenyl, acenaphthylene, acenaphthene, fluorene, phenanthrene, anthracene, xanthene, fluoranthene, pyrene, chrysene, phenol, cresols (o/p), 1-naphtol, 2-naphtol, benzofuran, dibenzofuran
Combusted solid carbon deposits (Tedlar gas bags)	Solid carbon deposits	C (assumed 100% C)
Unidentified condensable species	Undetected	Aliphatic hydrocarbon with more than four/five carbon atoms

The abovementioned calculation method is used to determine the global carbon balance for all the performed experiments. The yield of carbon-containing species is calculated as the %carbon

of the carbon content of the feedstock, which expresses the share of carbon-containing species in relation to the carbon balance. This provides a clear understanding of the carbon distribution among the products of steam cracking. Reporting the product yields as the %weight of the feedstock can be ambiguous, in particular for carbon oxides because the feedstock PE contains only carbon and hydrogen (see Table 2). The results reported in this work can be transformed to the %weight of the feedstock using the carbon and hydrogen contents of the feedstock for an unbiased comparison with the results reported in the literature. The undetected carbon reported here is the difference between the total carbon in the feedstock and the amounts of carbon measured in the products. The undetected carbon corresponds to the aliphatic hydrocarbon species with more than five carbon atoms, the detection of which was outside the scope of the analytical methods used in this work.

The yield of hydrogen gas (H_2) is reported in terms of its contribution to the overall hydrogen balance for each of the experiments. For the complete hydrogen balance, quantification of all individual paraffinic, olefinic and naphthenic species is required. However, as mentioned earlier, the quantification of individual C_3 , C_4 , and C_5 compounds was beyond the scope of the analytical methods used in this work. Therefore, instead of outlining the distribution of hydrogen atoms among the products of steam cracking, a range of H/C ratios of the products was determined. The calculated H/C ratios of the products was used as an indicator of the hydrogen transfer severity. For the purpose of determining the maximum value of the range, C_3H_x , C_4H_x , and C_5H_x were assumed to be C_3H_8 , C_4H_{10} , and C_5H_{12} , respectively, whereas for calculating the minimum value of the range, they were assumed to be C_3H_4 , C_4H_6 , and C_5H_8 , respectively. The yield of hydrogen gas (H_2) was not considered when calculating the ranges for the H/C ratios. Therefore, the H/C ratios calculated in this work correspond to carbon-containing species. Calculating the H/C ratio in this fashion also gives an indication of the amount of hydrogen that is retained by the carbon atoms of the feedstock.

CHAPTER 5

5 – Results and discussion

The results presented in this chapter are from the experimental work presented in **Papers I–III**. The results are divided into four topics, as summarized in Table 9.

Table 9. Experimental results covering the work presented in **Papers I–III**.

Investigation	Paper I	Paper II	Paper III
Properties of the bed materials	✓	✓	
Carbon balance	✓	✓	✓
Suitability of the feedstock	✓	✓	✓
H/C ratio of the products	✓	✓	

5.1 Properties of the bed materials

The presence of Fe in the synthesized bed materials $1\text{Fe}/\text{Al}_2\text{O}_3$, $2\text{Fe}/\text{Al}_2\text{O}_3$, and $5\text{Fe}/\text{Al}_2\text{O}_3$ was confirmed by SEM-EDS. The back-scattered electron (BSE) signal from a cross-section of the bed material $5\text{Fe}/\text{Al}_2\text{O}_3$ is shown in Figure 9. The contrast of the SEM images was developed using the variations in the average atomic weight of the elements present in the bed material sample. The brightness of the pixels increased with an increase in the atomic weight of the scanned element. As Fe is heavier than Al, the relative Fe content of the scanned sample can be determined from the BSE contrast. The micrographs acquired at higher magnification revealed that the surfaces of the particles exhibited a thin, bright layer rich in Fe. In addition, the EDS point analysis recorded for all the particles, as shown in Figure 9 (magnification:

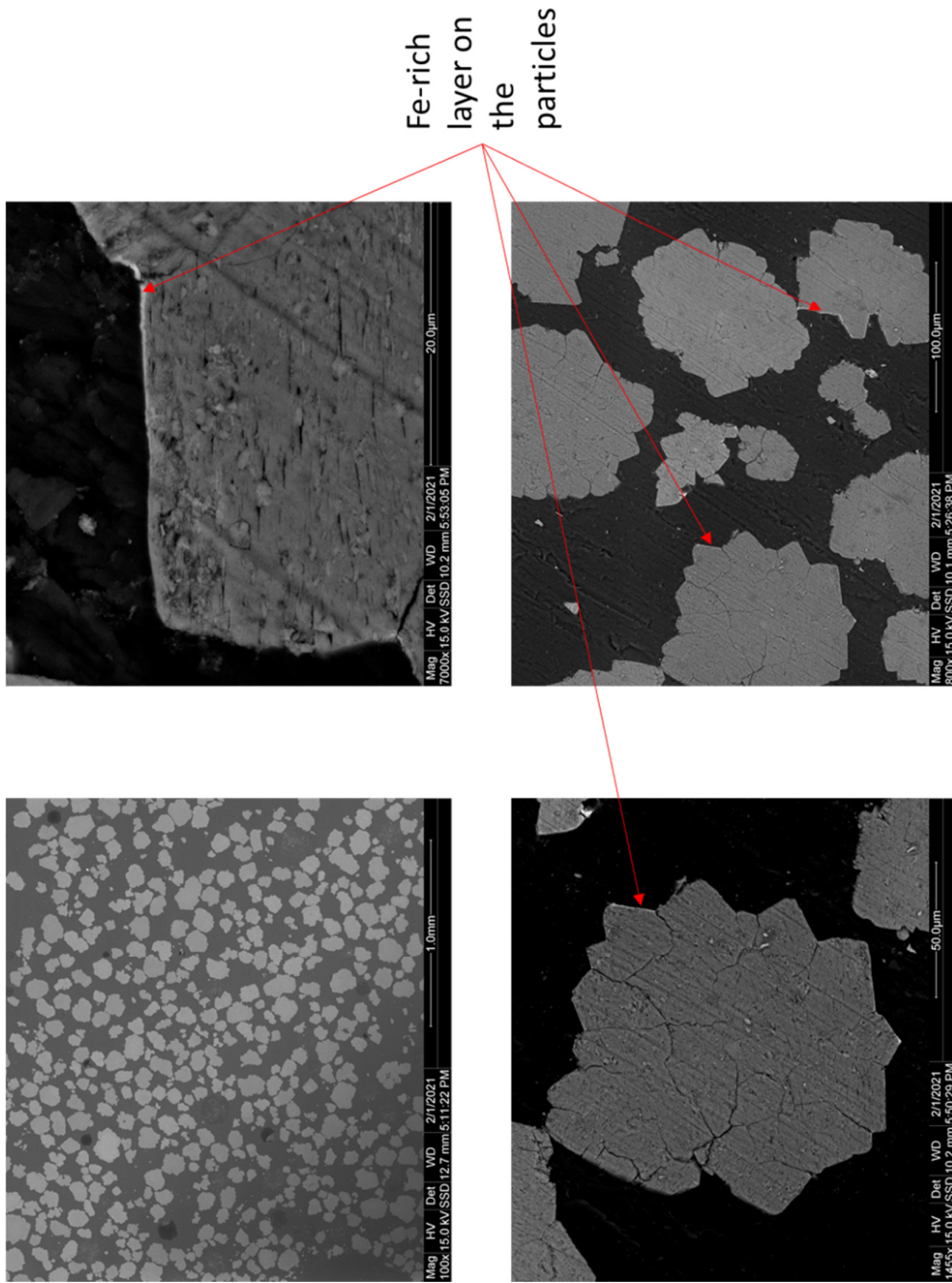


Figure 9. Back-scattered electron micrographs of the sample of the bed material 5Fe/Al₂O₃ with different magnification of the same SEM image.

100.0 μm) contained at least 1 atomic percentage (at.%) Fe. A similar analysis was performed for the samples of the bed materials $2\text{Fe}/\text{Al}_2\text{O}_3$ and $5\text{Fe}/\text{Al}_2\text{O}_3$. As expected, lower concentrations of Fe were found, and some particles only contained Fe close to the surface. Although Fe was unevenly distributed and some Al_2O_3 particles appeared to absorb preferentially large quantities of Fe, the presence of Fe was detected on the particle surfaces of all three samples.

The presence of Fe in the synthesized bed materials was further confirmed by measuring their oxygen transport capacities. Chemical looping tests were performed for the bed materials $1\text{Fe}/\text{Al}_2\text{O}_3$, $2\text{Fe}/\text{Al}_2\text{O}_3$, and $5\text{Fe}/\text{Al}_2\text{O}_3$ to measure their oxygen transport capacities. The oxygen transport capacity of Al_2O_3 was assumed to be 0 wt.%, since it contained <0.03 wt.% Fe_2O_3 (as described by the supplier).

Figure 10 shows the concentration profiles of CO and CO_2 , as logged by the permanent gas analyzer, during the reduction and the inert stages of the third chemical looping cycle for the $1\text{Fe}/\text{Al}_2\text{O}_3$, $2\text{Fe}/\text{Al}_2\text{O}_3$, and $5\text{Fe}/\text{Al}_2\text{O}_3$ bed materials. The first and the second cycles gave responses similar to those for the third cycle.

Based on the amount of CO converted to CO_2 by the bed material, the oxygen transport capacities (%w/w) of $1\text{Fe}/\text{Al}_2\text{O}_3$, $2\text{Fe}/\text{Al}_2\text{O}_3$, and $5\text{Fe}/\text{Al}_2\text{O}_3$ were estimated to be 0.25%, 0.32%, and 0.52%, respectively. The theoretical values for the oxygen transport capacities were estimated at 0.14 wt.%, 0.28 wt.%, and 0.71 wt.% (reduction from Fe_2O_3 to FeO) for $1\text{Fe}/\text{Al}_2\text{O}_3$, $2\text{Fe}/\text{Al}_2\text{O}_3$, and $5\text{Fe}/\text{Al}_2\text{O}_3$, respectively. The increase in oxygen transport capacity with the increasing iron content of the bed material ensures appropriate impregnation of Fe_2O_3 over Al_2O_3 .

The bed materials bauxite and olivine were used in the work performed in **Paper II**, considering their abilities to undergo redox cycles and drive the water dissociation reaction. The redox potentials of bauxite and olivine are attributed to their iron oxide contents (see Table 3). The water dissociation capabilities of bauxite and olivine, in their reduced forms, were determined by performing a blank test and quantifying the amount of hydrogen released by the bed material through oxidation by steam at 750°C . The concentration profile of the hydrogen gas released during the blank test was logged by the permanent gas analyzer and is shown in Figure 11.

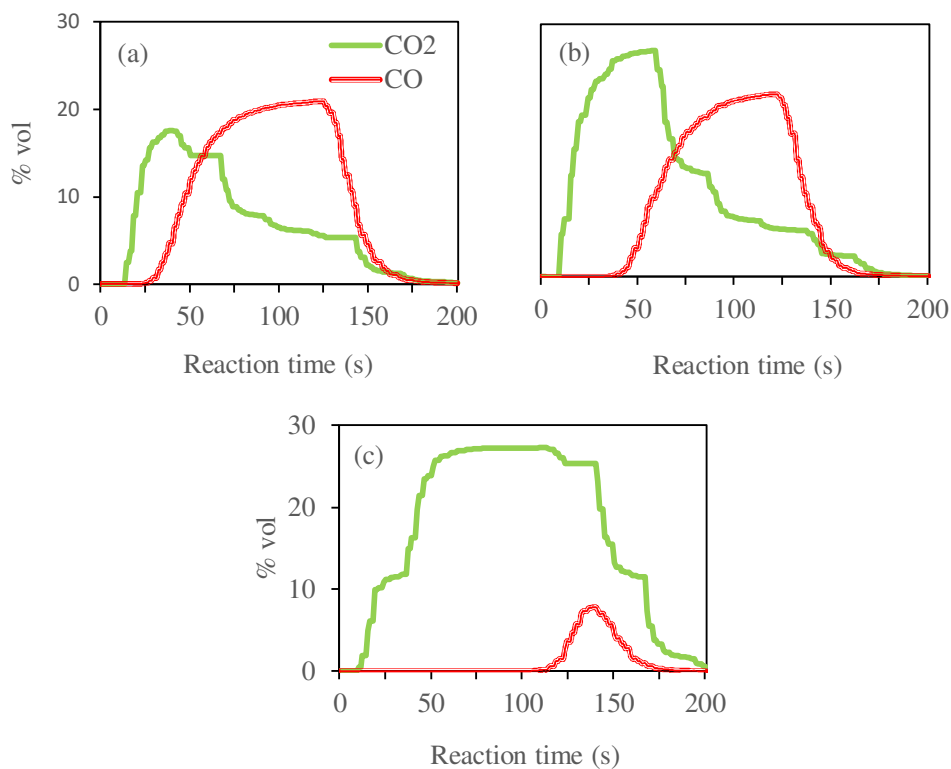


Figure 10. Measured concentrations of CO and CO₂ (%vol., dry) during the chemical looping tests of the bed materials: (a) 1Fe/Al₂O₃; (b) 2Fe/Al₂O₃; and (c) 5Fe/Al₂O₃.

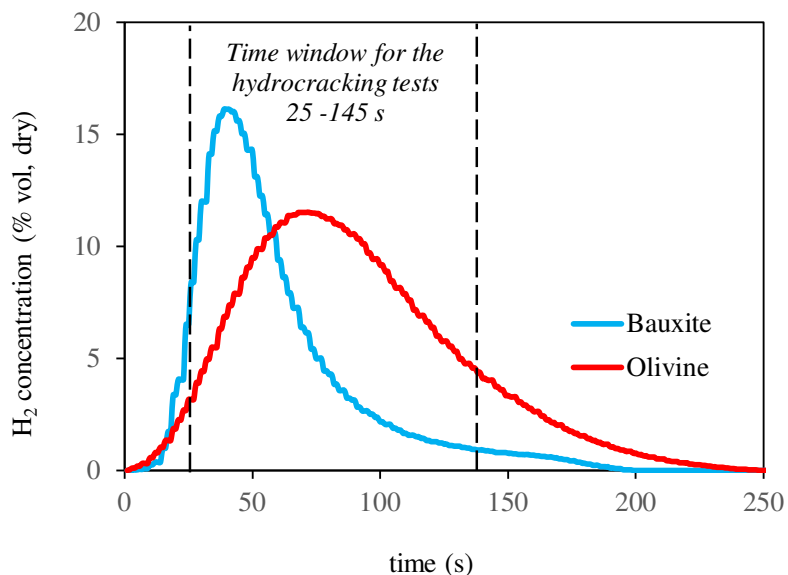


Figure 11. The concentration profile of hydrogen produced during the blank water dissociation tests with the bed materials bauxite and olivine. The time window of 25–145 s indicates the time period during which the hydrocracking tests were performed.

The total amounts of hydrogen (H₂) produced during the blank test were estimated as 0.013 mol and 0.019 mol for bauxite-H and olivine-H, respectively. The amounts of hydrogen produced during the indicated time window of 120 s corresponded to 0.012 mol and 0.017 mol for bauxite-H and olivine-H, respectively.

An investigation of the properties of the bed material silica sand was outside the scope of the present work. Silica sand was employed in **Paper III** and was assumed to be chemically inert towards the steam cracking reactions.

5.2 Carbon balance

Table 10 compares the product yields (%carbon and %hydrogen, by weight) obtained from the steam cracking experiments performed in **Papers I–III**. The results reported in Table 10 outline the overall carbon balance for all the performed experiments. The carbon balance closures obtained in this work fall in the range of 86%–97%. The undetected carbon reported in Table 10 represents the difference between the total carbon in the feedstock and the amount of carbon measured in the products. As previously mentioned, the undetected carbon corresponds to the aliphatic hydrocarbon species with more than four/five carbon atoms, the detection of which was beyond the scope of the analytic methods used in this work. The yield of hydrogen gas (H₂) is reported in terms of its contribution to the overall hydrogen balance.

Table 10. Distribution of obtained the products from the steam cracking experiments performed in this work.

	Al ₂ O ₃	1Fe/Al ₂ O ₃	2Fe/Al ₂ O ₃	5Fe/Al ₂ O ₃	bauxite	bauxite-H	olivine	olivine-H	RO650	RO700	RO750
<i>Olefins</i>	58.63	48.62	33.28	23.36	43.63	51.51	49.99	47.62	51.14	46.96	37.56
C ₂ H ₄	17.52	17.37	11.05	7.43	28.82	34.90	32.77	31.58	24.12	24.3	23.29
C ₃ H _x	11.08	11.27	6.85	4.38	10.25	11.17	12.9	12.59	16.76	14.55	9.3
C ₄ H _x + C ₅ H _x ^a	30.03	19.98	15.38	11.55	4.56	5.44	4.32	3.42	10.26	8.11	4.97
<i>Aromatics</i>	15.03	19.95	23.1	26.98	20.67	16.82	21.47	21.45	19.15	20.75	22.72
Benzene	6.06	8.26	10.19	11.41	10.42	8.78	10.99	11.3	7.67	8.73	10.81
Toluene	3.67	5.10	6.21	6.83	3.3	2.71	3.41	3.45	4.51	4.63	4.37
Xylenes	0.84	1.13	1.41	1.66	0.37	0.3	0.38	0.38	1.44	1.00	0.66
Styrene	0.84	1.11	1.46	1.58	1.60	1.16	1.65	1.46	1.30	1.63	1.76
Naphthalene	0.87	1.25	1.55	1.73	1.88	1.51	1.84	1.38	0.72	1.29	2.06
Others	2.73	3.10	2.28	3.77	3.09	2.36	3.19	3.02	3.51	3.49	3.06

<i>Paraffins</i>	13.73	12.95	9.29	6.26	14.44	18.34	15.75	16.94	12.86	14.22	14.92
CH ₄	8.95	8.30	6.27	4.35	10.98	13.59	11.87	12.52	6.80	8.64	10.06
C ₂ H ₆	4.78	4.65	3.02	1.91	3.46	4.75	3.88	4.42	6.06	5.57	4.86
<i>Carbon oxides</i>	4.70	5.77	10.32	13.53	4.90	4.22	4.63	5.61	11.57	11.82	17.24
CO	1.47	1.25	2.26	2.06	1.99	2.51	1.55	2.87	5.03	5.55	9.88
CO ₂	3.23	4.52	8.06	11.48	2.91	1.71	3.08	2.74	6.54	6.26	7.36
Solid carbon	2.19	6.59	12.08	15.50	2.64	1.08	0.82	1.31	2.17	1.90	1.70
Undetected ^b	5.72	6.14	11.93	14.37	13.72	8.03	7.14	7.10	3.11	4.35	5.87
H ₂ ^c	10.84	8.93	14.63	14.55	2.29	9.52	1.74	9.59	10.06	12.33	20.36

^a C₅H_x compounds were detected and measured only for Al₂O₃, 1Fe/Al₂O₃, 2Fe/Al₂O₃ and 5Fe/Al₂O₃.

^b Undetected represents the difference between the total carbon in the feedstock and the amount of carbon in the measured products.

^c The yield of H₂ is reported as its contribution (%) to the overall hydrogen balance.

5.3 Suitability of the feedstock

5.3.1 Polyethylene

The distribution of the products obtained from steam cracking of PE, under DFB operating conditions, was investigated in **Papers I** and **II**. Of the bed materials used in **Papers I** and **II**, Al₂O₃, bauxite, and olivine are assumed to have no or minimal influence on the bond scission reactions. The products obtained with the abovementioned bed materials are considered to be the outcomes of pure thermal cracking. Therefore, a fair comparison of the results obtained here can be made with the results for thermal cracking of petroleum naphtha.

Methane, ethane, ethylene, propylene, mono-aromatics (BTXS), and naphthalene were the main products obtained when using all three bed materials. The steam cracking temperatures were 700°C for Al₂O₃ and 750°C for bauxite and olivine. The product distribution, when going from the cracking temperature of 700°C (with Al₂O₃) to 750°C (with bauxite and olivine), followed the cracking severity trend described in Figure 3. A significant amount (30.03%) of C₄H_x and C₅H_x was obtained at the bed material temperature of 700°C. In contrast, the yields of C₄H_x at 750°C were 4.56% and 4.32% for the bed materials of bauxite and olivine, respectively. C₅H_x compounds were not detected in the product gas obtained at 750°C. A very low concentration of C₅ species in the product gas mixture could be one of the reasons why C₅ compounds were not detected in those experiments.

The decrease in the yield of heavy hydrocarbons (C₄H_x and C₅H_x) at higher temperature was linked to the formation of aromatic compounds and lighter hydrocarbons such as methane and ethylene. This is also in line with the trend for cracking severity described in Figure 3. The total yields (%carbon) of aromatic hydrocarbons increased from 15.03% at 700°C to 20.67% and 21.47% at 750°C (for bauxite and olivine, respectively). The yields of methane also increased when the temperature was increased from 700°C (8.95%) to 750°C (10.98% and 11.87%). The yields of ethylene were 17.52% at 700°C, 28.80% at 750°C (for bauxite), and 32.77% at 750°C (for olivine).

The product distribution obtained from the thermal cracking of polyolefin in this work is comparable to that obtained from the thermal cracking of petroleum naphtha.² In addition, the cracking severity trends for petroleum naphtha and polyethylene are closely related. As discussed earlier, this is mainly due to the similar molecular structures of naphtha and polyolefins. The results obtained in this work confirm that polyolefins are a suitable feedstock for a steam cracking process that is operated in a DFB reactor configuration.

5.3.2 Vegetable oil

The possibility to recover the carbon atoms of vegetable oil as molecular building blocks for the plastics industry was assessed in **Paper III**. The direct and indirect production levels of the molecular building blocks from the steam cracking of vegetable oil were considered. The products of steam cracking can be grouped, based on the recycling routes described in the *Landscape* of this thesis (Chapter 2), as follows: Route A (C₂H₄, C₂H₆, C₃H_x, C₄H_x, Benzene, Toluene, Xylenes, Styrene); Route B (H₂, CH₄, CO, CO₂); and Route C (Naphthalene, Other

aromatics, Coke, Undetected). The distributions of carbon atoms among the abovementioned groups, based on the results of the experiments performed in **Paper III**, are shown in Figure 12.

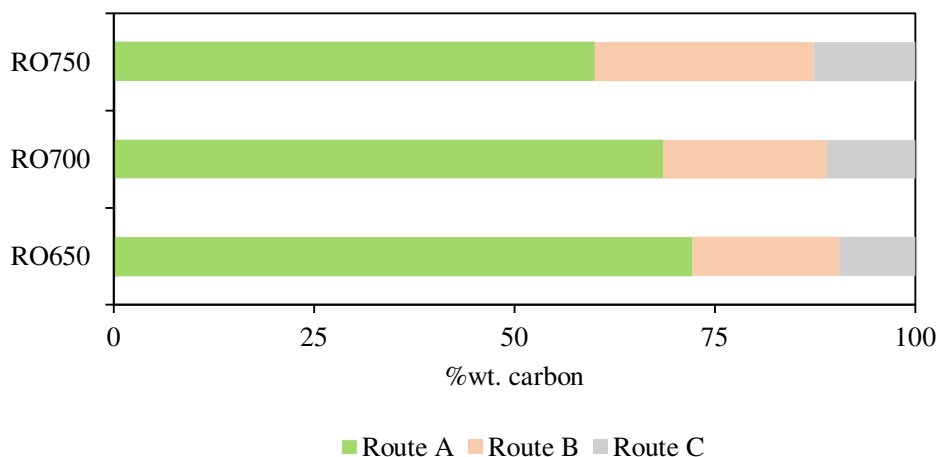


Figure 12. Distributions of carbon among the product groups, based on thermochemical recycling routes A, B and C (Route A: Direct production of petrochemical via steam cracking; Route B: Steam reforming followed by synthesis; Route C: Combustion followed by synthesis).

The direct production of the molecular building blocks was found to be strongly influenced by the temperature of the fluidized bed. The highest yield of 72.13% was obtained for the lowest bed material temperature of 650°C. Slightly lower yields of 68.53% and 60.02% were obtained at the bed material temperatures of 700°C and 750°C, respectively. The yields of molecular building blocks, at the higher temperatures, were reduced by the enhanced formation of CO, CO₂ and CH₄.

The CO, CO₂ and CH₄ obtained from the steam cracking of vegetable oil can be considered as raw syngas that can be sent for steam reforming and synthesis processes downstream of the steam cracker. The total yields of syngas were 18.37%, 20.46% and 27.29% for RO650, RO700, and RO750, respectively. The significant amount of carbon recovered as syngas underlines the desirability of conversion through the proposed Route B (recall Figure 2), whereby the syngas is converted to olefins to increase the recovery of carbon atoms as molecular building blocks. As discussed earlier, the production of the molecular building blocks through Route B will require additional hydrogen, depending on the R ratio of the produced syngas. The R ratios and the amounts of hydrogen required for the optimal production of methanol, downstream of the cracker, are presented in Figure 13. Conversion of syngas to olefins through Route B, downstream of the cracker, increases the carbon recovery rates to 90.50%, 88.99%, and 87.32% (as molecular building blocks), based on the product distributions obtained from the RO650, RO700, and RO750 tests, respectively.

The products, which include naphthalene, other aromatics, and solid carbon, together with the undetected aliphatic hydrocarbons (C₅+), can be converted into the molecular building blocks through Route C. Synthesis of the molecular building blocks through the complementary Route C will allow 100% recovery of the carbon atoms present in the feedstock.

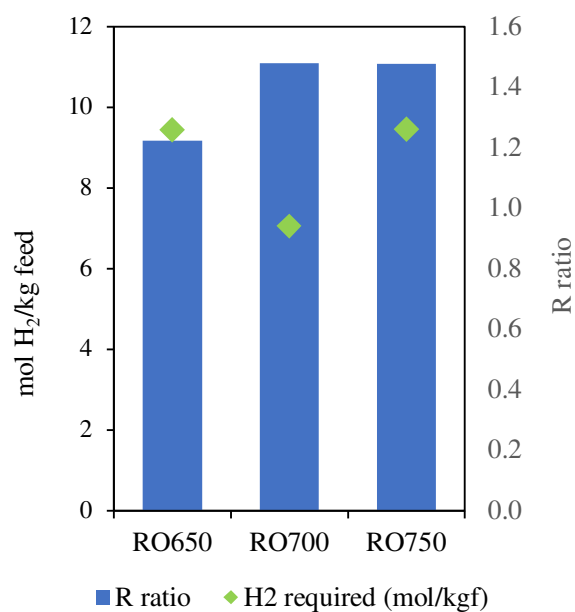


Figure 13. The R ratios of the syngas and the amounts of H₂ required to attain the optimal R ratio of 2 for each of the test series. The R ratio is defined as: $R = (H_2 - CO_2)/(CO + CO_2)$.

5.4 H/C ratio of the products

The average range of H/C ratio of the products was used as a tool to determine the hydrogen-transfer severity of the process. A higher hydrogen-transfer severity results in a greater deviation of the H/C ratio of the products from the H/C ratio of the feedstock (see Figure 5). The ranges of the H/C ratios of the products obtained from the experiments covered in **Papers I and II** are shown in Figure 14.

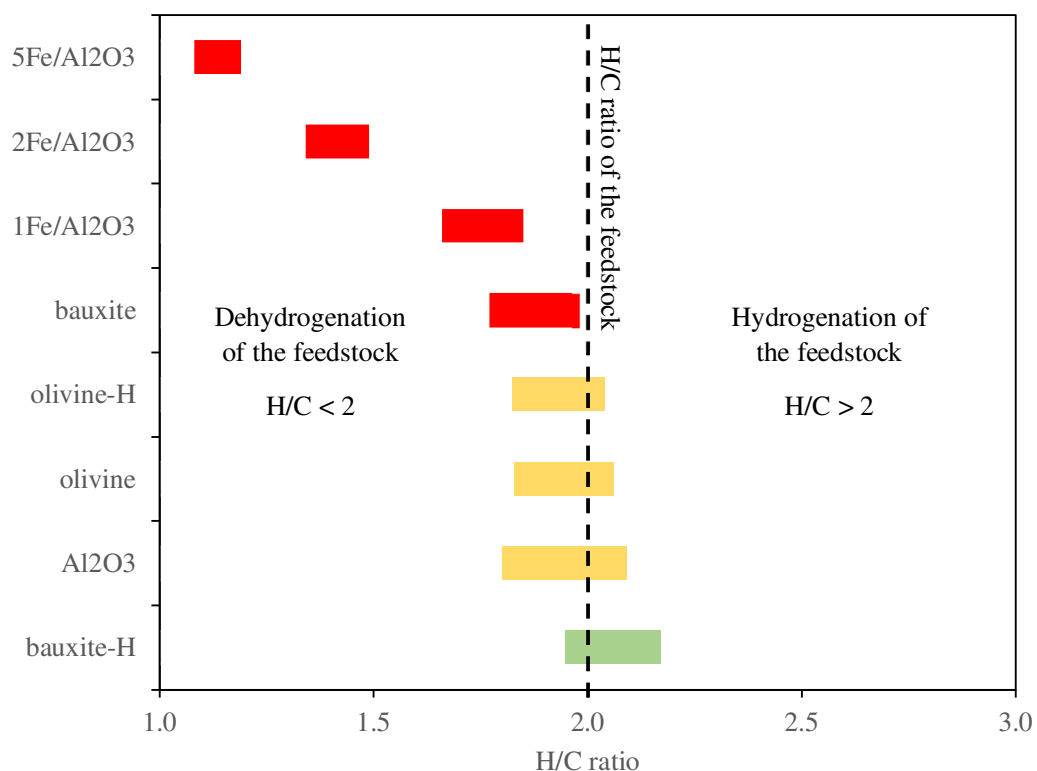


Figure 14. The range of the H/C ratio of the products obtained from the steam cracking experiments performed in **Papers I–III**.

It is evident from Figure 14 that the H/C ratio of the products and, consequently, the severity of the hydrogen transfer reactions are affected significantly by the bed materials. The initial feedstock PE molecule is composed of CH₂ repeating units and has an H/C ratio of 2. The increase in the hydrogen severity results in either dehydrogenation or hydrogenation of the feedstock. The H/C ratio of the products are similar to that of the feedstock when the hydrogen-transfer severity is lowest.

5.4.1 Dehydrogenation by the bed materials

The range of H/C ratios obtained with the bed materials 1Fe/Al₂O₃, 2Fe/Al₂O₃ and 5Fe/Al₂O₃ was significantly lower than 2. The H/C ratios of the products decreased with the increase in the iron oxide content of the bed material. In the absence of iron oxide in the bed material, i.e., Al₂O₃, the H/C ratios of the products (range, 1.8–2.1) were close to that of the initial PE molecule. The products derived using 5Fe/Al₂O₃, the bed material with the highest iron oxide content, showed the lowest H/C ratio range of 1.08–1.19. The decrease in the H/C ratio occurred mainly because the formation of aromatics, carbon oxides and carbon deposits was favored in the presence of bed materials that contained iron oxide (see Table 9).

The total yield of hydrogen atoms, including all the produced hydrocarbons and hydrogen gas (H_2), was also calculated for the abovementioned four bed materials. A trend similar to that presented in Figure 14 was observed for the total yield of hydrogen atoms. The yield of hydrogen atoms for the bed material Al_2O_3 was in the range of 95.4%–108.8%. The yields of hydrogen atoms for $1Fe/Al_2O_3$, $2Fe/Al_2O_3$, and $5Fe/Al_2O_3$ were significantly lower than that for Al_2O_3 . The trend for the total yield of hydrogen atoms is presented in Figure 15.

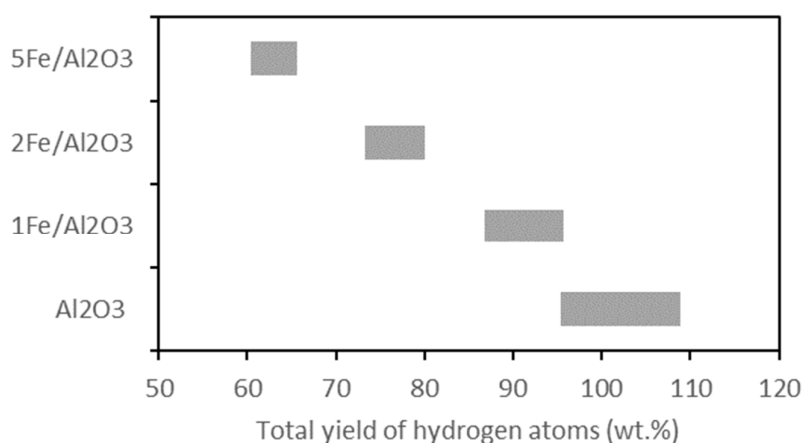


Figure 15. The total yield of hydrogen atoms for the bed materials Al_2O_3 , $1Fe/Al_2O_3$, $2Fe/Al_2O_3$ and $5Fe/Al_2O_3$.

The H/C ratios of the products and the total yield of hydrogen atoms indicate dehydrogenation of PE, followed by oxidation of the hydrogen atoms of the feedstock to H_2O . Dehydrogenation of PE by the bed material is analogous to the dehydrogenation of light paraffins in the CL-OHD process, as described in Chapter 2.

In the presence of a bed material that is capable of dehydrogenating polyolefin molecules, the initial polyolefin molecule is depleted of its hydrogen atoms before being broken down into smaller molecules. The oxidation of hydrogen atoms also indicates the possibility that there will be OH radical formation during the initial dehydrogenation step. The unstable OH radical is removed by removing one more H atom from the polyolefin chain or any other hydrocarbon molecule in the vicinity.

The product distribution derived from the cracking of a dehydrogenated polyolefin molecule can be explained in terms of the reaction mechanism described in Figure 16. The reaction mechanism proposed here is comparable to the reaction mechanism governing thermal degradation of dehydrochlorinated PVC due to the structural similarities between dehydrochlorinated PVC and dehydrogenated polyolefin molecules.^{72,73}

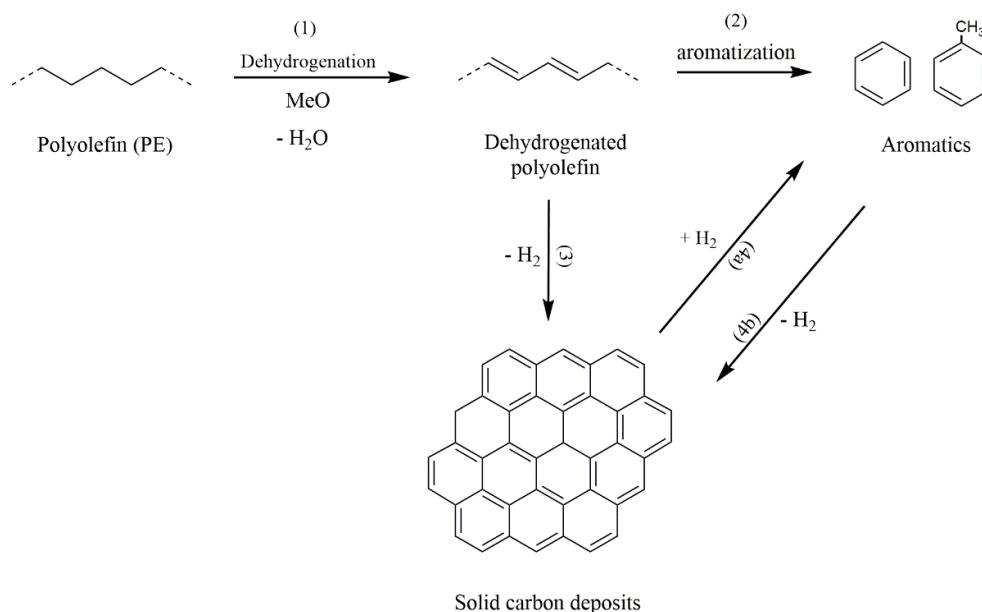


Figure 16. Reaction mechanism governing the formation of aromatics and solid carbon deposits from a dehydrogenated polyolefin molecule.

The formation of aromatic compounds proceeds through random scission of the dehydrogenated polyolefin molecule, followed by aromatization. The formation of the solid carbon deposits proceeds through two different routes: (1) random chain scission of the dehydrogenated polyolefin molecule with subsequent recombination into a mesh-like structure [reaction pathway (3) in Figure 16]; and (2) polymerization of the formed aromatic rings [reaction pathway (4b) in Figure 16]. In addition, random scission within the structure of the carbon deposits will also lead to the formation of aromatic rings [reaction pathway (4a) in Figure 16].

The reaction mechanism proposed here governs the product distribution mainly through the increase in hydrogen-transfer severity caused by the bed material. The hydrogen transfer reactions, in the form of dehydrogenation, are accelerated by the presence of iron oxide in the material. The finding that the formation of aromatics and carbon deposits is affected by the presence of iron oxide on the surface of the bed material is an indication that the proposed dehydrogenation step occurs exclusively on the surface of the bed material. Dehydrogenation of polyolefins, in a DFB steam cracking process, is expected when the bed material possesses and/or develops an oxygen transport capability.

5.4.2 Hydrogenation by the bed material

The range of H/C ratios of the products obtained with bauxite, olivine, and olivine-H was very close to the H/C ratio of the initial PE molecule (see Figure 14). This indicated that the hydrogen-transfer severity was low in the presence of these bed materials. The H/C ratios of the products obtained in the presence of bauxite-H were estimated to be in the range of 1.95–2.17. Bauxite-H was the only bed material used in this work that gave a product distribution

with H/C ratio significantly higher than that of the feedstock. This deviation also indicates the higher hydrogen-transfer severity in the presence of bauxite-H, as compared to the corresponding severities in the presence of bauxite, olivine, and olivine-H. However, in the case of bauxite-H, the higher hydrogen-transfer severity led to the hydrogenation of the feedstock, enhancing the production of molecules with H/C ratio ≥ 2 .

The increase in the H/C ratios of the products that occurred with bauxite-H as the bed material confirms the hydrogenation of the produced radical species by the hydrogen produced from the water dissociation reaction. The bed materials bauxite-H and olivine-H were employed to drive the water dissociation reaction in parallel with the steam cracking reaction. However, the water dissociation reaction in the presence of olivine-H exerted no influence on the produced free radical species, leading to a similar H/C ratio of the products as was obtained with olivine. The hydrogen generated from the water dissociation reaction on the surface of olivine-H was released entirely as H₂. This discrepancy can be explained by the differences between the two bed materials with respect to two critical parameters influencing the hydrogenation of free radicals during the hydrocracking process: (1) the hydrogen-donation capability of the surroundings; and (2) the hydrogen-transfer capability of the catalyst. These two parameters correspond to the hydrogen-donation capability of water and the hydrogen-transfer capability of the bed material (bauxite or olivine).

The hydrogen-donation capability of water is linked to the amount of hydrogen generated from the water dissociation reaction. The total amounts of hydrogen released by bauxite-H and olivine-H, as estimated from the blank water dissociation test, were 0.013 mol H₂ and 0.019 mol H₂, respectively. The finding of a similar yield of hydrogen from the blank water dissociation reaction confirmed that the hydrogen-donation capability of water was similar in the presence of either of the bed materials. Although the hydrogen-donation capability of water was similar in both cases, the hydrocracking phenomenon was observed exclusively with bauxite-H (see Figure 4). Therefore, it is evident that olivine-H does not have the ability to transfer the generated hydrogen to the hydrocarbon species, leading to H/C ratios of the products similar to those seen with olivine.

In conventional hydrocracking processes, the ability of the catalyst to transfer the hydrogen to the hydrocarbon species is linked to the surface availability of the active sites and the characteristics of the catalyst support.⁵² The bed materials used in this work are not identical to the hydrocracking catalysts, although some similarities can be drawn between them. The reduced iron present in bauxite-H and olivine-H, which facilitates the water dissociation reaction, can be considered as the active site. The remainder of the bed material, which remains inactive towards the water dissociation reaction, can be considered the support for the active site.

The surface availability of active sites can be considered similar for bauxite-H and olivine-H, bearing in mind the similar water dissociation capabilities of the two materials. The other parameter that affects the hydrogen-transfer capability of the catalyst is the catalyst support. For the conventional hydrocracking catalysts, the catalyst support is made up of amorphous silica-alumina, zeolite, or a combination of both of these materials.⁵² These support materials are ideally porous, offering a large surface area for catalytic reactions. Some properties of bauxite, in this case, are comparable to that of a conventional hydrocracking catalyst support.

Bauxite contains the basic components of a hydrocracking catalyst support, i.e., aluminum oxide (Al_2O_3) and silicon dioxide (SiO_2). The bauxite used in this work had a combined Al_2O_3 and SiO_2 concentration of 93 wt.% (see Table 1). In addition, bauxite is known to have a porosity similar to those of the hydrocracking catalyst supports.^{74,75} Given these properties of bauxite, it has also been used to prepare high-efficiency hydrocracking catalyst supports.^{74,75} On the other hand, olivine has no properties corresponding to those of a hydrocracking catalyst support. Olivine, being a magnesium silicate, is known to contain negligible concentrations of free Al_2O_3 and SiO_2 .^{76,77} Therefore, the ability of bauxite to transfer the hydrogen generated from the water dissociation reaction to the hydrocarbon species can be attributed to the reasons discussed here.

It is clear from the above discussion that water dissociation reaction (by the active sites) in a fluidized bed steam cracking process has the potential to hydrogenate the produced hydrocarbon free radicals. The use of bed materials (bauxite and olivine) with different properties revealed that the overall hydrocracking potential of fluidized beds depends on the hydrogen-transfer capability of the bed material. However, the influences of the bed material properties, such as the chemical composition, porosity and the surface density of the active sites, on the hydrogen transfer potential of the bed material, the examination of which was beyond the scope of this work, need to be determined.

The hydrogenation effect observed here requires a continuous water dissociation reaction in the steam cracker. However, once the bed material is oxidized by steam it can no longer sustain the water dissociation reaction. In addition, the bed material entering the steam cracker will be fully oxidized due to the oxidizing environment in the regenerator of the DFB steam cracker. Therefore, continuous reduction of the bed material is required before it comes in contact with the plastic waste stream. Figure 17 shows a modified DFB reactor configuration that enables reduction of the bed material after the regenerator, thereby sustaining the water dissociation reaction in the steam cracker.

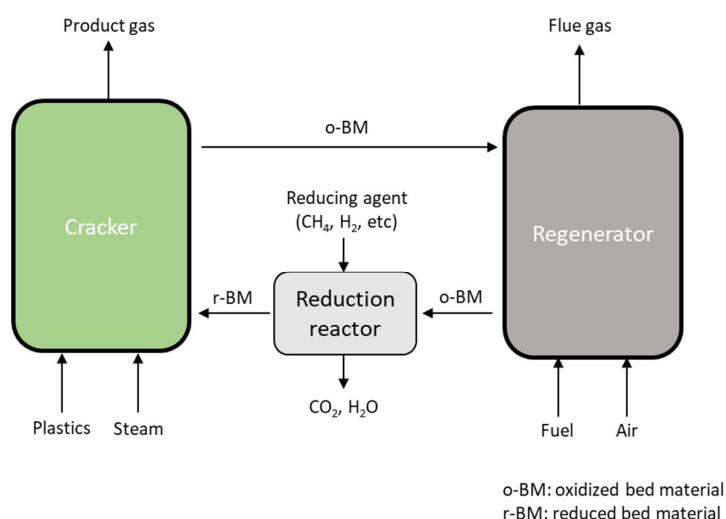


Figure 17. Schematic of a DFB steam cracker that enables continuous reduction of the bed material before entry into the steam cracker.

CHAPTER 6

6 – Summary and Conclusions

Steam cracking of polyolefins in a DFB reactor configuration is a promising alternative to the recycling of abundantly available plastic wastes. Steam cracking of polyolefins enables the production of the molecular building blocks that can be used to manufacture new plastic materials of the same quality as those manufactured from fossil reserves. The development of such a technology for polyolefin plastic materials is critical for meeting the challenge of depleting fossil reserves and for the management of plastic wastes. The experimental work presented in this thesis revolves around strengthening the value of the DFB system compared the other plastic recycling technologies. The primary aim was to investigate the suitability of the DFB steam cracking process for polyolefin and polyolefin-type feedstocks. PE was selected as a model polyolefin feedstock and rapeseed oil was chosen as a model polyolefin-type feedstock. The investigation determined the effects of the operational conditions in a DFB system on the reaction mechanism related to the steam cracking of polyolefins. In particular, the investigation focused on determining how the bed material influences the hydrogen transfer reactions and, thereby, the product distribution. The investigation of the hydrogen transfer reactions was complemented with an experimental evaluation of six different bed materials. In total, three experimental studies were conducted using a laboratory-scale bubbling fluidized bed reactor that resembles the steam cracker of a DFB system.

The main outcomes of this thesis are summarized below.

- The results obtained in this work confirm that a DFB steam cracking process is suitable for the production of the molecular building blocks for the plastics industry. The product distributions obtained from steam cracking of polyolefin and polyolefin-type feedstocks are comparable to those obtained from the thermal cracking of petroleum naphtha. The cracking severities for vegetable oil and polyethylene also follow the same trend as that for naphtha.

- Investigation of the steam cracking of vegetable oil revealed that vegetable oils, and subsequently, WCO represent suitable feedstocks for the plastic recycling system. Up to 51% of light olefins, 15% of mono-aromatics, and 13% of light paraffins were recovered as products of the steam cracking process.
- The product distributions obtained in this work are comparable to those obtained from the thermal cracking of naphtha only when the bed material shows minimal catalytic activity towards the hydrogen transfer reactions.
- Increasing the activity of the bed material towards the hydrogen transfer reactions results in either the dehydrogenation or hydrogenation of polyolefins. As such, dehydrogenation leads to the formation of solid carbon deposits, aromatics, and polycyclic aromatic hydrocarbons, while hydrogenation leads to the enhanced formation of hydrocarbons with H/C ratios ≥ 2 , including light olefins and paraffins.
- Dehydrogenation by the bed material is linked to the oxidizing nature of the bed material. Dehydrogenation by the bed material proceeds through oxidation of the hydrogen atoms of the polyolefin polymer chain, followed by the formation of carbon-to-carbon double bonds along the polymer chain. Subsequent cracking of the polymer chain with carbon-to-carbon double bonds leads to the formation of compounds with H/C ratios < 2 .
- The dehydrogenation of polyolefins by the bed material is observed through the formation of OH radicals, which are subsequently removed as H₂O after abstraction of H atoms from the polymer chain or other hydrocarbon species in the vicinity. The proposed dehydrogenation step is found to take place exclusively on the surface of the bed material.
- Hydrogenation by the bed material is associated with the hydrogen-donation capability of water and the hydrogen-transfer capability of the bed material. The enhanced formation of hydrocarbons with H/C ratios ≥ 2 arises from hydrogenation of the unstable free radicals produced from the steam cracking reactions. This also leads to suppression of the formation of aromatics and PAHs.
- The hydrogen-donation capability of the water molecules is governed by the extent of the water dissociation reaction, which is driven by the reducing properties of the bed material. The released hydrogen atoms are then transferred to the free radical species to complete the hydrogenation reaction.
- The transfer of the hydrogen atoms is, however, dependent upon the bed material. Of the two reduced bed materials tested, bauxite and olivine, hydrogenation was observed exclusively in the presence of reduced bauxite.

Recommendations for future work

The results obtained in this work underline the importance of the DFB steam cracking process for thermochemical recycling of plastic waste. The experimental results also point to several issues that warrant further investigation in the context of the further development of such a recycling process.

The products of steam cracking included in the carbon balance closure were limited by the sampling and analytic techniques employed in this work. An evaluation of economically valuable hydrocarbons, such as individual C₄ olefins and other aliphatic hydrocarbons, would further strengthen the standing of such a recycling system.

Furthermore, investigations of large-scale DFB systems that are likely to develop oxygen transport capabilities are desirable. Such investigations will require a systematic experimental campaign in which a DFB steam cracker is fed with feedstocks that contribute to the oxidizing properties of the bed material.

The use of reduced bauxite and olivine with different properties revealed that hydrogenation of the free radicals depends on the hydrogen-transfer capability of the bed material. The impacts of the bed material properties, such as the chemical composition, porosity and the surface density of the active sites, on the hydrogen transfer potentials of the bed materials were beyond the scope of this work but need to be elucidated.

Finally, the investigation of the steam cracking of vegetable oil opens up new avenues for the conversion of different biogenic waste streams, such as WCO and animal fat. Despite the possibilities for producing the molecular building blocks for plastics from WCO, WCO has found application in the biofuels industry. Nevertheless, in a scenario in which the consumption of fossil-based resources is phased out and the transportation sector is electrified, it will be justifiable to develop recycling methods such as those proposed in this work. The development of such processes will require further investigation of the impacts of impurities present in real-life WCO on the steam cracking process and the processes that lie downstream.

Nomenclature

MMT	<i>metric million tonnes</i>
LPG	<i>liquefied petroleum gas</i>
WFD	<i>waste framework directive</i>
PET	<i>polyethylene terephthalate</i>
FCC	<i>fluid catalytic cracking</i>
DFB	<i>dual fluidized bed</i>
WCO	<i>waste cooking oil</i>
MTO	<i>methanol-to-olefins</i>
PE	<i>polyethylene</i>
PP	<i>polypropylene</i>
PVC	<i>polyvinyl chloride</i>
PS	<i>polystyrene</i>
BTXS	<i>benzene toluene xylenes styrene</i>
PMMA	<i>polymethyl methacrylate</i>
HDPE	<i>high-density polyethylene</i>
CLG	<i>chemical looping gasification</i>
CL-OHD	<i>chemical looping oxidative dehydrogenation</i>
CLC	<i>chemical looping combustion</i>
ASR	<i>automotive shredder residue</i>
FA	<i>fatty acids</i>
USFA	<i>unsaturated fatty acids</i>
SFA	<i>saturated fatty acids</i>
BFB	<i>bubbling fluidized bed</i>
MFC	<i>mass flow controller</i>
SPE	<i>solid-phase extraction</i>
SEM	<i>scanning electron microscope</i>
EDS	<i>energy-dispersive x-ray spectroscopy</i>
SPA	<i>solid-phase adsorption</i>
GC	<i>gas chromatography</i>
FID	<i>flame ionization detector</i>
BSE	<i>backscattered electron</i>
M_o	<i>mass of oxygen released by bed material</i>
M_b	<i>initial mass of bed material</i>
n_i	<i>molar yield of I, in mol/kg</i>
c_i	<i>concentration of I, in %vol</i>
C_{He}	<i>concentration of helium, in %vol</i>
m_f	<i>mass of feedstock, in kg</i>
V_{He}	<i>volume of tracer helium, in l</i>
C_{He}	<i>concentration of helium, in %vol</i>
V_m	<i>volume of an ideal gas at STP, in l/m</i>

References

1. Plastics Europe (2020). EU plastics production and demand - first estimates for 2020 :: PlasticsEurope. Association of Plastics Manufacturers.
2. Thunman, H., Berdugo Vilches, T., Seemann, M., Maric, J., Vela, I.C., Pissot, S., and Nguyen, H.N.T. (2019). Circular use of plastics-transformation of existing petrochemical clusters into thermochemical recycling plants with 100% plastics recovery. *Sustainable Materials and Technologies* 22.
3. Geyer, R., Jambeck, J.R., and Law, K.L. (2017). Production, use, and fate of all plastics ever made. *Science Advances* 3.
4. European Parliament and Council (2008). Waste Framework Directive. Official Journal of the European Union.
5. Kutz, M. (2016). *Applied Plastics Engineering Handbook: Processing, Materials, and Applications: Second Edition*.
6. Kaminsky, W. (2021). Chemical recycling of plastics by fluidized bed pyrolysis. *Fuel Communications* 8.
7. Wilk, V., and Hofbauer, H. (2013). Conversion of mixed plastic wastes in a dual fluidized bed steam gasifier. *Fuel* 107.
8. Maric, J., Berdugo Vilches, T., Thunman, H., Gyllenhammar, M., and Seemann, M. (2018). Valorization of Automobile Shredder Residue Using Indirect Gasification. *Energy and Fuels* 32.
9. Gamble, A. (2019). *Ullmann's Encyclopedia of Industrial Chemistry*. The Charleston Advisor 20.
10. Davis, B.H. (2003). Fischer-Tropsch synthesis: Relationship between iron catalyst composition and process variables. In *Catalysis Today*.
11. Kaminsky, W., and Mennerich, C. (2001). Pyrolysis of synthetic tire rubber in a fluidised-bed reactor to yield 1,3-butadiene, styrene and carbon black. *Journal of Analytical and Applied Pyrolysis* 58–59.
12. Larsson, A., Kuba, M., Berdugo Vilches, T., Seemann, M., Hofbauer, H., and Thunman, H. (2021). Steam gasification of biomass – Typical gas quality and operational strategies derived from industrial-scale plants. *Fuel Processing Technology* 212.
13. Karl, J., and Pröll, T. (2018). Steam gasification of biomass in dual fluidized bed gasifiers: A review. *Renewable and Sustainable Energy Reviews* 98.
14. Levine, S.E., and Broadbelt, L.J. (2009). Detailed mechanistic modeling of high-density polyethylene pyrolysis: Low molecular weight product evolution. *Polymer Degradation and Stability* 94.

15. Marongiu, A., Faravelli, T., and Ranzi, E. (2007). Detailed kinetic modeling of the thermal degradation of vinyl polymers. *Journal of Analytical and Applied Pyrolysis* 78.
16. Mastral, J.F., Berruero, C., and Ceamanos, J. (2007). Modelling of the pyrolysis of high density polyethylene. Product distribution in a fluidized bed reactor. *Journal of Analytical and Applied Pyrolysis* 79.
17. Tian, P., Wei, Y., Ye, M., and Liu, Z. (2015). Methanol to olefins (MTO): From fundamentals to commercialization. *ACS Catalysis* 5.
18. Stöcker, M. (1999). Methanol-to-hydrocarbons: Catalytic materials and their behavior. *Microporous and Mesoporous Materials* 29.
19. Atsbha, T.A., Yoon, T., Seongho, P., and Lee, C.J. (2021). A review on the catalytic conversion of CO₂ using H₂ for synthesis of CO, methanol, and hydrocarbons. *Journal of CO₂ Utilization* 44.
20. Behrens, M., Studt, F., Kasatkin, I., Kühl, S., Hävecker, M., Abild-Pedersen, F., Zander, S., Girgsdies, F., Kurr, P., Knief, B.L., et al. (2012). The active site of methanol synthesis over Cu/ZnO/Al₂O₃ industrial catalysts. *Science* (1979) 336.
21. Marlin, D.S., Sarron, E., and Sigurbjörnsson, Ó. (2018). Process Advantages of Direct CO₂ to Methanol Synthesis. *Frontiers in Chemistry* 6.
22. Kaminsky, W., Schlesselmann, B., and Simon, C. (1995). Olefins from polyolefins and mixed plastics by pyrolysis. *Journal of Analytical and Applied Pyrolysis* 32.
23. Li, S., Cañete Vela, I., Järvinen, M., and Seemann, M. (2021). Polyethylene terephthalate (PET) recycling via steam gasification – The effect of operating conditions on gas and tar composition. *Waste Management* 130.
24. Yu, J., Sun, L., Ma, C., Qiao, Y., and Yao, H. (2016). Thermal degradation of PVC: A review. *Waste Management* 48.
25. Mosher, M. (1992). *Organic Chemistry*. Sixth edition (Morrison, Robert Thornton; Boyd, Robert Neilson). *Journal of Chemical Education* 69.
26. Orsavova, J., Misurcova, L., Vavra Ambrozova, J., Vicha, R., and Mlcek, J. (2015). Fatty acids composition of vegetable oils and its contribution to dietary energy intake and dependence of cardiovascular mortality on dietary intake of fatty acids. *International Journal of Molecular Sciences* 16.
27. Statista (2021). • Worldwide production major vegetable oils, 2012-2021 | Statista. <https://www.statista.com/statistics/263933/production-of-vegetable-oils-worldwide-since-2000/>.
28. Orsavova, J., Misurcova, L., Vavra Ambrozova, J., Vicha, R., and Mlcek, J. (2015). Fatty acids composition of vegetable oils and its contribution to dietary energy intake and dependence of cardiovascular mortality on dietary intake of fatty acids. *International Journal of Molecular Sciences* 16.
29. USDA (2021). *Oilseeds: World Markets and Trade*. Foreign Agricultural Service/USDA.

30. Loizides, M.I., Loizidou, X.I., Orthodoxou, D.L., and Petsa, D. (2019). Circular bioeconomy in action: Collection and recycling of domestic used cooking oil through a social, reverse logistics system. *Recycling* 4.
31. Gui, M.M., Lee, K.T., and Bhatia, S. (2008). Feasibility of edible oil vs. non-edible oil vs. waste edible oil as biodiesel feedstock. *Energy* 33.
32. Hsiao, M.-C., Liao, P.-H., Lan, N.V., and Hou, S.-S. (2021). Enhancement of Biodiesel Production from High-Acid-Value Waste Cooking Oil via a Microwave Reactor Using a Homogeneous Alkaline Catalyst. *Energies (Basel)* 14, 437.
33. Sarno, M., and Iuliano, M. (2019). Biodiesel production from waste cooking oil. *Green Processing and Synthesis* 8.
34. Meira, M., Quintella, C.M., Ribeiro, E.M.O., Silva, H.R.G., and Guimarães, A.K. (2015). Overview of the challenges in the production of biodiesel. *Biomass Conversion and Biorefinery* 5.
35. Muhbat, S., Tufail, M., and Hashmi, S. (2021). Production of diesel-like fuel by co-pyrolysis of waste lubricating oil and waste cooking oil. *Biomass Conversion and Biorefinery*.
36. Yusuff, A.S., Thompson-Yusuff, K.A., and Igbafe, A.I. (2022). Synthesis of biodiesel via methanolysis of waste frying oil by biowaste-derived catalyst: process optimization and biodiesel blends characterization. *Biomass Conversion and Biorefinery*.
37. Aatola, H., Larmi, M., Sarjovaara, T., and Mikkonen, S. (2009). Hydrotreated vegetable Oil (HVO) as a renewable diesel fuel: Trade-off between NO_x, particulate emission, and fuel consumption of a heavy duty engine. *SAE International Journal of Engines* 1.
38. Bezergianni, S., and Kalogianni, A. (2009). Hydrocracking of used cooking oil for biofuels production. *Bioresource Technology* 100.
39. Bezergianni, S., Voutetakis, S., and Kalogianni, A. (2009). Catalytic hydrocracking of fresh and used cooking oil. *Industrial and Engineering Chemistry Research* 48.
40. Maafa, I.M. (2021). Pyrolysis of polystyrene waste: A review. *Polymers (Basel)* 13.
41. Cerqueira, H.S., Caeiro, G., Costa, L., and Ramôa Ribeiro, F. (2008). Deactivation of FCC catalysts. *Journal of Molecular Catalysis A: Chemical* 292.
42. Miskolczi, N., Bartha, L., and Deák, G. (2006). Thermal degradation of polyethylene and polystyrene from the packaging industry over different catalysts into fuel-like feed stocks. In *Polymer Degradation and Stability*.
43. Achilias, D.S., Roupakias, C., Megalokonomos, P., Lappas, A.A., and Antonakou, V. (2007). Chemical recycling of plastic wastes made from polyethylene (LDPE and HDPE) and polypropylene (PP). *Journal of Hazardous Materials* 149.
44. Lee, K.H., Jeon, S.G., Kim, K.H., Noh, N.S., Shin, D.H., Park, J., Seo, Y., Yee, J.J., and Kim, G.T. (2003). Thermal and Catalytic Degradation of Waste High-density

- Polyethylene (HDPE) Using Spent FCC Catalyst. *Korean Journal of Chemical Engineering* 20.
45. Elordi, G., Olazar, M., Castaño, P., Artetxe, M., and Bilbao, J. (2012). Polyethylene cracking on a spent FCC catalyst in a conical spouted bed. *Industrial and Engineering Chemistry Research* 51.
 46. de La Puente, G., Klocker, C., and Sedran, U. (2002). Conversion of waste plastics into fuels recycling polyethylene in FCC. *Applied Catalysis B: Environmental* 36.
 47. Mandviwala, C., Berdugo Vilches, T., Seemann, M., Faust, R., and Thunman, H. (2022). Thermochemical conversion of polyethylene in a fluidized bed: Impact of transition metal-induced oxygen transport on product distribution. *Journal of Analytical and Applied Pyrolysis* 163.
 48. Mertinkat, J., Kirsten, A., Predel, M., and Kaminsky, W. (1999). Cracking catalysts used as fluidized bed material in the Hamburg pyrolysis process. *Journal of Analytical and Applied Pyrolysis* 49.
 49. Pissot, S., Berdugo Vilches, T., Maric, J., Cañete Vela, I., Thunman, H., and Seemann, M. (2019). Thermochemical Recycling of Automotive Shredder Residue by Chemical-Looping Gasification Using the Generated Ash as Oxygen Carrier. *Energy and Fuels* 33.
 50. Zhu, X., Imtiaz, Q., Donat, F., Müller, C.R., and Li, F. (2020). Chemical looping beyond combustion-a perspective. *Energy and Environmental Science* 13.
 51. Yu, Z., Yang, Y., Yang, S., Zhang, Q., Zhao, J., Fang, Y., Hao, X., and Guan, G. (2019). Iron-based oxygen carriers in chemical looping conversions: A review. *Carbon Resources Conversion* 2.
 52. Saab, R., Polychronopoulou, K., Zheng, L., Kumar, S., and Schiffer, A. (2020). Synthesis and performance evaluation of hydrocracking catalysts: A review. *Journal of Industrial and Engineering Chemistry* 89.
 53. Munir, D., Irfan, M.F., and Usman, M.R. (2018). Hydrocracking of virgin and waste plastics: A detailed review. *Renewable and Sustainable Energy Reviews* 90.
 54. Munir, D., Irfan, M.F., and Usman, M.R. (2018). Hydrocracking of virgin and waste plastics: A detailed review. *Renewable and Sustainable Energy Reviews* 90.
 55. Alemán-Vázquez, L.O., Cano-Domínguez, J.L., and García-Gutiérrez, J.L. (2012). Effect of tetralin, decalin and naphthalene as hydrogen donors in the upgrading of heavy oils. In *Procedia Engineering*.
 56. Hart, A., Lewis, C., White, T., Greaves, M., and Wood, J. (2015). Effect of cyclohexane as hydrogen-donor in ultradispersed catalytic upgrading of heavy oil. *Fuel Processing Technology* 138.
 57. Zhang, Z., Chen, H., Wang, C., Chen, K., Lu, X., Ouyang, P., and Fu, J. (2018). Efficient and stable Cu-Ni/ZrO₂ catalysts for in situ hydrogenation and deoxygenation of oleic acid into heptadecane using methanol as a hydrogen donor. *Fuel* 230.

58. Matuszewska, A., Hańderek, A., Biernat, K., and Bukrejewski, P. (2019). Thermolytic Conversion of Waste Polyolefins into Fuels Fraction with the Use of Reactive Distillation and Hydrogenation with the Syngas under Atmospheric Pressure. *Energy and Fuels* 33.
59. Hosseinpour, M., Ahmadi, S.J., and Fatemi, S. (2016). Deuterium tracing study of unsaturated aliphatics hydrogenation by supercritical water in upgrading heavy oil. Part I: Non-catalytic cracking. *Journal of Supercritical Fluids* 107.
60. Fedyaeva, O.N., and Vostrikov, A.A. (2012). Hydrogenation of bitumen in situ in supercritical water flow with and without addition of zinc and aluminum. *Journal of Supercritical Fluids* 72.
61. Hosseinpour, M., Fatemi, S., and Ahmadi, S.J. (2015). Catalytic cracking of petroleum vacuum residue in supercritical water media: Impact of α -Fe₂O₃ in the form of free nanoparticles and silica-supported granules. *Fuel* 159.
62. Sato, T., Sumita, T., and Itoh, N. (2015). Effect of CO addition on upgrading bitumen in supercritical water. *Journal of Supercritical Fluids* 104.
63. Hosseinpour, M., Fatemi, S., and Ahmadi, S.J. (2016). Deuterium tracing study of unsaturated aliphatics hydrogenation by supercritical water in upgrading heavy oil. Part II: Hydrogen donating capacity of water in the presence of iron(III) oxide nanocatalyst. *Journal of Supercritical Fluids* 110.
64. Gladine, C., Meunier, N., Blot, A., Bruchet, L., Pagès, X., Gaud, M., Floter, E., Metin, Z., Rossignol, A., Cano, N., et al. (2011). Preservation of micronutrients during rapeseed oil refining: A tool to optimize the health value of edible vegetable oils? Rationale and design of the Optim'Oils randomized clinical trial. *Contemporary Clinical Trials* 32.
65. Gunstone, F.D. (2011). *Vegetable Oils in Food Technology: Composition, Properties and Uses*, Second Edition.
66. BATISTA, A.C.F., VIEIRA, A.T., RODRIGUES, H.S., SILVA, T.A., ASSUNÇÃO, R.M.N., BELUOMINI, M.A., REZENDE, H.P., and HERNANDEZ-TERRONES, M.G. (2014). PRODUCTION AND PHYSICOCHEMICAL CHARACTERIZATION OF METHYLIC AND ETHYLIC BIODIESEL FROM CANOLA OIL. *Revista Brasileira de Engenharia de Biosistemas* 8.
67. Dupain, X., Costa, D.J., Schaverien, C.J., Makkee, M., and Moulijn, J.A. (2007). Cracking of a rapeseed vegetable oil under realistic FCC conditions. *Applied Catalysis B: Environmental* 72.
68. Israelsson, M., Seemann, M., and Thunman, H. (2013). Assessment of the solid-phase adsorption method for sampling biomass-derived tar in industrial environments. *Energy and Fuels* 27.
69. Zhang, H., Nie, J., Xiao, R., Jin, B., Dong, C., and Xiao, G. (2014). Catalytic co-pyrolysis of biomass and different plastics (polyethylene, polypropylene, and polystyrene) to improve hydrocarbon yield in a fluidized-bed reactor. In *Energy and Fuels*.

70. Elordi, G., Olazar, M., Lopez, G., Artetxe, M., and Bilbao, J. (2011). Product yields and compositions in the continuous pyrolysis of high-density polyethylene in a conical spouted bed reactor. *Industrial and Engineering Chemistry Research* 50.
71. Jung, S.H., Cho, M.H., Kang, B.S., and Kim, J.S. (2010). Pyrolysis of a fraction of waste polypropylene and polyethylene for the recovery of BTX aromatics using a fluidized bed reactor. *Fuel Processing Technology* 91.
72. Zhou, J., Liu, G., Wang, S., Zhang, H., and Xu, F. (2020). TG-FTIR and Py-GC/MS study of the pyrolysis mechanism and composition of volatiles from flash pyrolysis of PVC. *Journal of the Energy Institute* 93.
73. Gui, B., Qiao, Y., Wan, D., Liu, S., Han, Z., Yao, H., and Xu, M. (2013). Nascent tar formation during polyvinylchloride (PVC) pyrolysis. *Proceedings of the Combustion Institute* 34.
74. Yue, Y., Li, J., Dong, P., Wang, T., Jiang, L., Yuan, P., Zhu, H., Bai, Z., and Bao, X. (2018). From cheap natural bauxite to high-efficient slurry-phase hydrocracking catalyst for high temperature coal tar: A simple hydrothermal modification. *Fuel Processing Technology* 175.
75. Yue, Y., Niu, P., Jiang, L., Cao, Y., and Bao, X. (2016). Acid-Modified Natural Bauxite Mineral as a Cost-Effective and High-Efficient Catalyst Support for Slurry-Phase Hydrocracking of High-Temperature Coal Tar. *Energy and Fuels* 30.
76. Faust, R., Berdugo Vilches, T., Malmberg, P., Seemann, M., and Knutsson, P. (2020). Comparison of Ash Layer Formation Mechanisms on Si-Containing Bed Material during Dual Fluidized Bed Gasification of Woody Biomass. *Energy and Fuels* 34.
77. Devi, L., Craje, M., Thüne, P., Ptasinski, K.J., and Janssen, F.J.J.G. (2005). Olivine as tar removal catalyst for biomass gasifiers: Catalyst characterization. *Applied Catalysis A: General* 294.